11-23-2016

Dopamine Effects of Stimulant and Non-Stimulant drugs used in the Treatment of Attention Deficit Hyperactivity Disorder

Preeti Chalwadi
Illinois State University, preeti.chalwadi1986@gmail.com

DOPAMINE EFFECTS OF STIMULANT AND NON-STIMULANT DRUGS USED IN THE TREATMENT OF ATTENTION DEFICIT HYPERACTIVITY DISORDER

Preeti Chalwadi

74 Pages

Attention deficit hyperactivity disorder (ADHD) is thought to be associated with dysfunction of ascending catecholamine neuronal systems, particularly dopamine (DA) and norepinephrine (NE). Dysfunction of these catecholamine neurons innervating the prefrontal cortex is hypothesized to underlie impaired executive functions. Dysfunction of the DA neurons innervating the striatum is additionally hypothesized to underlie deficits in motivation and reinforcement learning. However, mechanisms of action of therapeutic drugs used for treating ADHD have mainly focused on catecholamines in the prefrontal cortex and have not adequately addressed the role played by DA signaling in the striatum. Stimulants such as Adderall® and Ritalin® are chemically considered “amphetamines”. While effective for treating ADHD, there are grave concerns about stimulant abuse with this drug class. The more recently developed Strattera®, a non-stimulant used to treat AHDH, offers a non-addictive alterative. However, how Strattera® acts pharmacologically in the brain is not completely established. Our study investigates the brain mechanisms of Strattera® and specifically examines how Strattera® acts on brain dopamine neurons, which are important for learning. The second part of the study investigates the mechanism of action of the stimulant class of drugs. Stimulants act on brain dopamine neurons by blocking a protein that removes dopamine after its release to terminal neurotransmission. This action is thought to underlie the addictive potential of stimulants. We are

pursuing a novel action of stimulants: increasing the dopamine released by action potential dependent exocytosis. This action would increase brain dopamine, thereby mediating some of the pharmacological effects of stimulants. Collectively, our studies provide insight into how important drugs used clinically and often are abused act on the brain. The long-term goal is to distinguish the clinically efficacious component of these drugs from their addictive potential, which should help drive development of safer drugs for treating ADHD.

KEYWORDS: Dopamine; Atomoxetine; Psychostimulants; Amphetamine; Modafinil; Cocaine; Phasic dopamine signaling; Transients; DAT-inhibitor.

DOPAMINE EFFECTS OF STIMULANT AND NON-STIMULANT DRUGS USED IN THE TREATMENT OF ATTENTION DEFICIT HYPERACTIVITY DISORDER

PREETI CHALWADI

A Dissertation Submitted in Partial
Fulfillment of the Requirements
for the Degree of

DOCTOR OF PHILOSOPHY

School of Biological Sciences

ILLINOIS STATE UNIVERSITY

2017

DOPAMINE EFFECTS OF STIMULANT AND NON-STIMULANT DRUGS USED IN THE TREATMENT OF ATTENTION DEFICIT HYPERACTIVITY DISORDER

PREETI CHALWADI

COMMITTEE MEMBERS:

Paul A. Garris, Chair

Craig Gatto

Wolfgang Stein

Joe Casto

Byron Heidenreich

ACKNOWLEDGMENTS

I would like to express my heartfelt gratitude towards my advisor, Dr. Paul Garris, for being an excellent mentor. I thank him for his immense patience and constant encouragement throughout the course of my PhD studies. His intellectual brilliance is matched only by his genuinely good nature and his humility. I could not have asked for a better advisor.

I would also like to thank my committee members, Drs. Craig Gatto, Wolfgang Stein, Joe Casto, and Byron Heidenreich, for their insightful questions and comments for my research work, and for the general collegiality each of them offered to me over the years. My sincere thanks to Dr. Craig Gatto, who as department chair, helped me move through various obstacles during my PhD with much ease.

I thank all members of the Garris lab present during my graduate career, who proved an invaluable resource for my growth as a graduate student. In particular, I am grateful to Doug Schuweiler, Martin Bobak, Matthew Weber, and Melissa Doellman, who taught me the experimental procedures necessary to carry out the research.

I also wish to express my thanks to Mrs. Khushie Curmally, for leaving no stone unturned in her efforts to ensure that I meet my educational goals in the USA without feeling burdened. I am overwhelmed by her compassion and generosity. I would be remiss not to mention the invaluable support of my friends Niket Bhodia, Aditi Vyas, and Suranjana Sen, who have stood by me through thick and thin over the years, showing great love and graciousness. In a similar vein, I would like to acknowledge Sarita Sharma, Aditya Airen, Dheeraj Reddy, Saket Jangle, Akanksha Shukla, and Aditya Bennuri for their kindness and for helping me tide through some challenging times.

I owe my success, in a large way, to my family. Most importantly, I am grateful to my mother, Anu Chalwadi, for her innumerable sacrifices in bringing me up to be where I am today. Her love has been my biggest strength as I pursued this final degree. My grandparents, Mr. Hanumanta Chalwadi and Mrs. Gangamma Chalwadi, have always been with me in spirit throughout my dissertation and my life in general. I am also tremendously thankful to my uncles Nityanand Chalwadi, Sukmani Chalwadi, Mallesh Chalwadi, and Gangadhar Penta whose support and protection have been a blessing for me.

P.C.

CONTENTS

CHAPTER I FIGURES

CHAPTER II FIGURES

CHAPTER II SUPPLEMENTARY FIGURES

CHAPTER I

EFFECT OF ATOMOXETINE ON PHASIC DOPAMINE SIGNALING

Abstract

Attention deficit hyperactivity disorder (ADHD) is thought to be associated with dysfunction of ascending catecholamine systems in the brain, particularly dopamine (DA) and norepinephrine (NE). Dysfunction of these catecholamine neurons innervating the prefrontal cortex is hypothesized to underlie impaired executive functions. Dysfunction of the DA neurons innervating the striatum is additionally hypothesized to underlie deficits in motivation and reinforcement learning. However, investigating mechanisms of action of therapeutic drugs used for treating ADHD has mainly focused on catecholamines in the prefrontal cortex and have not adequately addressed the role played by DA signaling in the striatum. The present study addresses this issue by examining the neuropharmacologic mechanism of atomoxetine (ATX), a potent and selective NE reuptake inhibitor, on phasic DA signaling in the striatum of anesthetized rats. ATX, a non-stimulant approved for ADHD treatment in the form of Strattera®, is suggested to produce its therapeutic effects by enhancing catecholamine transmission in the prefrontal cortex. We propose that in addition to its remedial effects in the prefrontal cortex, ATX enhances phasic DA signaling in the striatum. We found ATX to activate DA transients, the extracellular component of phasic DA signaling occurring in DA terminal fields and elicited by burst firing of DA neurons, which were measured by fast-scan cyclic voltammetry at a carbon-fiber microelectrode. This study is neurobiologically significant, because it leads to a better understanding of the role NE plays in regulating phasic DA signaling in the striatum. Moreover, this study sheds light on the incompletely understood therapeutic mechanism of action of ATX and hence, may contribute towards development of better drugs for treating ADHD.

Introduction

Attention deficit hyperactivity disorder (ADHD) is a neurodevelopmental disorder with an onset in childhood and can continue into adolescence and adulthood. 5% of the children in the United States have ADHD (American Psychiatric Association, 2013). According to the DSM-5, ADHD is characterized by insufficient levels of attention and high levels of impulsivity and hyperactivity. These symptoms have been linked to deficits in executive function, response inhibition, and reinforcement learning, which in turn result from an underlying brain dysfunction, particularly the prefrontal cortex (PFC) and the striatum. While the PFC is involved in executive functions, such as inhibition of inappropriate behavior, planning, organization, and attention (Arnsten & Li, 2005), the striatum is important in processing reward-related information (Apicella et al., 1991; Kawagoe et al., 1998). Various imaging studies have pointed towards hypo-functional PFC (Castellanos et al., 1996) and striatal activity as pivotal pathophysiologic features of ADHD (Aston-Jones et al., 2000; Lou et al., 1989). The catecholamines, specifically dopamine (DA) and norepinephrine (NE), and their dysfunctional modulation of the prefrontal and striatal circuits are the principal neuropharmacologic target in treating ADHD (Castellanos & Tannock, 2002).

Models of ADHD pathophysiology include the inverted-U model, which describes PFC function and dysfunction using an inverted-U dose-response curve for both DA and NE (Levy, 2009). It hypothesizes that in individuals with ADHD, catecholamines are present at lower than optimal levels. Low catecholamine levels result in an underactive PFC, due to diminished activation of the D1 and α-2 adrenergic receptors by DA and NE, respectively (Aston-Jones et al., 2000; Arnsten & Pliszka, 2011). Another model, called the dopamine transfer deficit (DTD) model, addresses the role of the striatum in ADHD. The DTD model describes a neuronal mechanism whereby ADHD patients show altered reinforcement learning, during which the

reward (reinforcer) becomes associated with a predictive cue over time (Berridge, 2001). Early in reinforcement learning, the DA transient, an extracellular phasic signal initially elicited by the reward activating burst firing of DA neurons (Schultz, 1998), is transferred in part, to the predictive stimulus, but it also remains activated by the reward itself. Later in learning, the DA transient is solely elicited by the predictive cue (Tripp & Wickens, 2008). The DTD model proposes that in individuals with ADHD, this transfer of the DA transient from the reward to the cue is disturbed, such that the cue-evoked DA transient is weak, leading to ineffective reinforcement learning (Tripp & Wickens, 2008).

Medications approved by the Food and Drug Administration for treating ADHD include psychostimulants, such as amphetamine (AMPH; Adderall) and methylphenidate (MPH; Ritalin), and more recently, a non-stimulant, atomoxetine (ATX; Strattera®) (Bymaster et al., 2002). All of these ADHD drugs increase extracellular NE and DA concentrations in the brain by blocking their uptake; specifically, AMPH and MPH block the NE transporter (NET) and the DA transporter (DAT), whereas ATX selectively inhibits NET. In terms of therapeutic implications of the inverted-U model, it is suggested that ADHD drugs elevate extracellular levels of DA and NE in the PFC and hence, improve PFC functionality (Arnsten, 2006). Microdialysis studies show that ATX, AMPH, and MPH increase NE and DA levels in the PFC (Bymaster et al., 2002; Berridge & Stalnaker, 2002; Berridge & Stalnaker, 2002; Berridge & Stalnaker, 2002). While AMPH and MPH also increase extracellular DA in the striatum (Kuczenski & Segal, 2001; Berridge et al., 2006), ATX does not (Bymaster et al., 2002). Taken together, these results suggest that ADHD drugs elicit these catecholamine effects preferentially, and in the case of ATX, exclusively, in the PFC. However, microdialysis has limited temporal resolution, preventing the

assessment of the effects of these drugs on DA transients (Borland et al., 2005; Robinson et al., 2003), whose dysfunction is implicated in the DTD model of ADHD.

Work in anesthetized rats suggests that ADHD drugs also activate burst firing of DA neurons. For example, *in vivo* electrophysiological recordings have shown AMPH and MPH to elicit burst firing of VTA DA neurons (Shi et al., 2004). AMPH-induced burst firing of DA neurons was blocked following administration of the α1 NE antagonist, prazosin (Shi et al., 2000; Shi et al., 2004). Furthermore, AMPH administration failed to produce burst firing of DA neurons following a forebrain hemisection, severing neuronal projections from the PFC to the midbrain (Shi et al., 2004). Taken together, these results suggest that NE is an important mediator of the DA effects of psychostimulants and that PFC afferents to the VTA contribute to eliciting burst firing of the DA neurons. High-affinity NET inhibitors such as nisoxetine and reboxetine, which increase PFC NE levels, also activate DA neuron burst firing (Shi et al., 2000; Linner et al., 2001). Thus, ADHD medications may elicit their therapeutic effects, at least in part, through activation of DA neuron burst firing facilitated by increased NE levels and α-1 receptor activation in the PFC. This activation of DA cell burst firing should in turn give rise to DA transients in the ventral striatum, a hypothesis not tested to date.

Previous work in our lab using fast-scan cyclic voltammetry (FSCV) at a carbon-fiber microelectrode (CFM), which exhibits the requisite temporal and chemical resolution to monitor DA transients with high fidelity (Roberts et al., 2013), has shown AMPH to elicit DA transients in the striatum (Daberkow et al., 2013; Ramsson et al., 2011; Covey et al., 2013). Whether ATX also elicits DA transients in this brain region is not known. Psychostimulant ADHD drugs, such as AMPH, also have presynaptic effects at DA terminals. Not only do they decrease DA uptake, in keeping with their well-recognized role as DAT inhibitors, but recent evidence suggests that

they also increase exocytotic DA release (Covey et al., 2013; Daberkow et al., 2013). In the present study, we thus wanted to investigate whether ATX similarly alters presynaptic DA mechanisms and DA transients in the striatum. Here we use FSCV at a CFM to monitor electrically evoked phasic-like DA signals and DA transients. We also used this analytical technique coupled to a chemometrics approach to monitor changes in basal DA levels in the striatum in order to compare with previous microdialysis measurements characterizing ATX action. We found that ATX activates DA transients in the ventral striatum without altering presynaptic DA mechanisms, as reflected by electrically evoked phasic-liked DA signals and basal DA levels. Taken together, our results suggest that in addition to increasing PFC levels of DA and NE, ATX activates phasic DA signaling in the striatum, which could be a novel mechanism mediating its therapeutic efficacy in treating ADHD.

Materials and Methods

Animals

Adult Sprague-Dawley rats (350-500g) were purchased from Harlan (Indianapolis, IN, USA) and housed in a light- and temperature-controlled vivarium. Access to food and water was provided *ad libitum*. All procedures were in accordance with the *National Institutes of Health Guide for the Care and Use of Laboratory Animals* and were approved by the Institutional Animal Care and Use Committee of Illinois State University.

Surgery

Adult male Sprague-Dawley rats were anesthetized with urethane (1.6 g/kg, i.p.) and mounted in a stereotaxic apparatus. An incision of the scalp was made, and skin and fascia removed. Holes for reference, stimulating, and recording electrodes were drilled through the skull. All coordinates, anteroposterior (AP), mediolateral (ML) and dorsoventral (DV), are given in mm

and are referenced to bregma (Paxinos & Watson, 2007). The stimulating electrode was placed in the medial forebrain bundle (MFB; -4.6 AP, +1.3 ML, -7.5 DV), a CFM targeted the ipsilateral ventral striatum (+1.2 AP, +1.5 ML, -6.5 DV), and the Ag/AgCl reference electrode was placed superficially in the contralateral cortex. Final positions of the CFM and stimulating electrode were based on optimizing the electrically evoked DA signal and were fixed for the duration of the experiment.

Experimental design

As shown in Figure 1, two experimental designs were used in the present study. In both designs, DA signals were recorded in 5-min epochs and when applied, electrical stimulation occurred 5 s into the epoch. Design 1 was used for a pilot set of experiments with drugs administered i.p. (Fig. 1A). In Design 1a, three pre-drug epochs were followed by twelve ATX (10 mg/kg), twelve RAC (0.2 mg/kg), and thirteen AMPH (10 mg/kg; administered along with a second dose of RAC (0.2 mg/kg); positive control) epochs. The order of RAC and ATX administration was reversed for Design 1b. Electrical stimulation was applied into each pre-drug epoch, and 30- and 60-min post-drug epochs. These epochs were analyzed for electrically evoked phasic-like DA signals and DA transients. Figure 1B shows Design 2, which was used for the remainder of the experiments with drugs administered i.v. In Design 2a, three pre-drug epochs were followed by two saline (SAL, negative control), two ATX (10 mg/kg), two raclopride (RAC, 0.1 mg/kg), and three AMPH (1 mg/kg; positive control) epochs. The order of RAC and ATX administration was reversed for Design 2b. Electrically evoked phasic-like DA signals, DA transients, and changes in basal DA levels were evaluated for each epoch.

Electrochemistry

DA was recorded using FSCV at a CFM (Roberts et al., 2013). A triangular waveform (-0.4 to 1.3 V and back, 400 V/s) was applied to the CFM every 100 ms. CFMs were prepared by aspirating a single carbon fiber (r = 2.5 μm) into a borosilicate capillary tube (1.2 mm o.d.; Sutter Instruments, Novato, CA, USA) and pulling to a taper using a micropipette puller (Narishige, Tokyo, Japan). The carbon fiber was then cut to ~100 μm distal to the glass seal. A Universal Electrochemistry Instrument (Department of Chemistry Electronic Shop, University of North Carolina, Chapel Hill, NC, USA) and commercially available software (ESA, Chelmsford, MA, USA) were used to perform FSCV. CFMs were calibrated in a modified TRIS buffer (Kume-Kick & Rice, 1998; Wu et al., 2001) after each experiment to convert the current recorded at the peak oxidative potential for DA (~+0.6 V) to concentration (Wightman et al., 2007). DA was initially identified by the background subtracted voltammogram (Michael et al., 1998; Heien et al., 2004). In experiments assessing effects of MOD on basal DA and DA transients, DA was additionally identified using principal component regression (PCR; see below).

Electrical stimulation

Biphasic stimulation pulses (2 ms each phase) were applied to a twisted bipolar stimulating electrode (Plastics One, Roanoke, VA, USA), with tips spaced ~1 mm apart. Stimulus pulses were optically isolated and constant current (Neurolog NL800; Digitimer Limited, Letchworth Garden City, UK), and delivered as 60-Hz, 24-pulse trains with a current intensity of ±300 μA.

Data analysis

Figures 1C and D conceptually describe data analyses. To quantify changes in basal DA (Δ[DA]) and DA transients, the FSCV record was first processed by PCR to resolve DA from the interferents, pH and background drift (Howard et al., 2013; Covey et al., 2016). PCR-resolved epochs were accepted if any current not accounted for by the retained principal components of the training sets, or residual (Q), was less than the 95% confidence threshold (Qα). Δ[DA] was calculated by averaging all data in the PCR-resolved DA trace of each 5-min epoch after the baseline has stabilized following electrical stimulation and noise artifacts generated by drug injection (Fig. 1C, right and left panels). DA transients in the PCR record were identified as peaks in the non-electrically evoked record greater than 5-times the root-mean-square noise, using peak-finding software (Mini-Analysis, Synaptosoft, Decatur, GA) (Fig. 1C, INSET). The maximal amplitude of electrically evoked phasic-like DA signals ($[DA]_{max}$) was analyzed to quantify drug effects on presynaptic DA mechanisms (Fig. 1D). $[DA]_{max}$ was determined from the raw FSCV, because at short times DA is the predominant analyte monitored by FSCV with MFB stimulation (see Fig. 1C).

Statistics

When appropriate, data are presented as the mean ± SEM. One-way repeated-measures ANOVA, with time or drug as the factor and repeated measures, was used to assess drug effects on $[DA]_{max}$, DA transients, and Δ[DA]. Post-hoc comparisons employed the Sidak test. All statistical analyses were performed using SAS, and significance was set at $p < 0.05$.

Drugs and chemicals

Atomoxetine hydrochloride was kindly provided by the Lilly Research Laboratories, Indianapolis, IN. Raclopride and D-amphetamine were purchased from Sigma (St. Louis, MO, USA).

Results

I.p. drug administration

Pilot experiments assessing i.p. drug administration were performed using Design 1 shown in Figure 1A. The order of drug administration in Design 1a (n = 2) was ATX, RAC, and AMPH. The order of ATX and RAC was reversed in Design 1b (n = 2). Figure 2A shows representative FSCV recordings demonstrating the effects of ATX, RAC, and AMPH on electrically evoked phasic-like DA signals measured in the ventral striatum. These evoked DA responses recorded under pre-drug conditions are considered phasic-like, because they emulate the amplitude and dynamics of naturally occurring DA transients (Robinson et al., 2008). The individual voltammogram (INSET in each panel) and pseudo-color plot displaying all voltammograms collected during the measurement in time (below each [DA] versus time recording) indicate that DA was the predominate analyte evoked by MFB stimulation for pre-drug and drug conditions. Compared to the pre-drug recording, RAC increased the maximal amplitude of the electrically evoked DA signal ($[DA]_{max}$) and its duration. While ATX did not alter $[DA]_{max}$ or the dynamics of this signal, AMPH further enhanced its $[DA]_{max}$ and duration.

Drug effects on $[DA]_{max}$ were analyzed by combining the time series of $[DA]_{max}$ (i.e., repeating 5-min epochs) into drug groups, as shown in Figure 2B. One-way repeated measures ANOVA with pseudo-replication was performed and revealed significant effects of drug on $[DA]_{max}$ for Design 1a ($F_{3,3} = 56.53$, $p = 0.0039$). Post-hoc tests revealed no significant increase

in $[DA]_{max}$ with ATX (p = 1.0), whereas both RAC (p = 0.047) and AMPH ($p < 0.0001$) significantly increased $[DA]_{max}$ compared to pre-drug control. Consistent with representative recordings, Design 2 showed a significant effect of drug ($F_{3,3} = 81.55$, $p = 0.0023$), and post-hoc tests showed that RAC significantly increased $[DA]_{max}$ ($p < 0.0001$), but ATX and AMPH did not bring about any further increase. Taken together, the results suggest that ATX administered i.p. either in the presence or absence of RAC does not alter electrically evoked phasic-like DA signals recorded in the ventral striatum.

We also failed to detect any DA transients in response to ATX or RAC with i.p. administration, as shown in the representative recordings in Figure 2C. Only AMPH, which was used as a positive control, and when co-administered with a second dose of RAC, elicited DA transients. Similar results were found across all animals in Design 1a and Design 1b. While the lack of presynaptic DA effects of ATX in the striatum was expected, the lack of ATX effects on DA transients was not and could be due to slow drug adsorption with the i.p. route of administration. Because drug adsorption is about twice as high for i.v. of administration (Woodard, 1965), we investigated ATX effects with this route using Designs 2a and 2b (Figure 1B, n = 4 and 4, respectively) for the remainder of the study.

ATX does not alter electrically evoked phasic-like DA signals

Figure 3A shows representative recordings demonstrating the effects of SAL, ATX, RAC, and AMPH on electrically evoked phasic-like DA responses measured in the ventral striatum following i.v. administration and using Design 2a. The individual voltammograms (INSET in each panel) and pseudo-color plot displaying all voltammograms collected during the measurement in time (below each [DA] versus time recording) indicate that DA is the predominant analyte evoked by MFB stimulation for pre-drug and drug conditions. ATX did not alter $[DA]_{max}$ or the dynamics

of the evoked response compared to SAL. In contrast, both RAC and AMPH increased $[DA]_{max}$ and its duration. AMPH appeared to further enhance the RAC-altered evoked response.

Figure 3B shows average values of $[DA]_{max}$ for each 5 min-epoch and expressed as a percent change from the pre-drug condition. One-way repeated measures ANOVA revealed a significant effect of time for Design 2a (left panel; $F_{11,44} = 9.02$, $p < 0.0001$) and Design 2b (right panel; $F_{11,33} = 4.78$, $p = 0.0002$). To further analyze drug effects, the time series of $[DA]_{max}$ shown in each 5-min epoch was compiled into drug groups in Figure 3C. Because post-hoc tests revealed no significant differences between pre-drug and SAL groups, a single control for $[DA]_{max}$ was created by combining both groups. One-way repeated measures ANOVA with pseudo-replication revealed a significant effect of drug on $[DA]_{max}$ for Design 2a (left panel; $F_{3,56} = 32.14$, $p < 0.0001$). Post-hoc tests revealed no significant increase in $[DA]_{max}$ with ATX ($p = 0.7786$), whereas both RAC ($p = 0.0001$) and AMPH ($p < 0.0001$) significantly increased $[DA]_{max}$ compared to control and ATX. A significant effect of drug was also found for Design 2b (right panel; $F_{3,32} = 10.57$, $p < 0.0001$), and post-hoc tests showed that while RAC significantly increased $[DA]_{max}$ ($p = 0.0055$), ATX and AMPH did not bring about any further increase. Thus, consistent with i.p. administration, i.v. ATX did not alter electrically evoked phasic-like DA signals. Taken together, these results suggest that ATX does not act presynaptically on striatal DA terminals.

ATX activates DA transients

Figure 4A shows representative recordings demonstrating the effects of SAL, ATX, RAC, and AMPH on DA transients in the ventral striatum following i.v. administration and using Design 2a. Each panel shows a PCR-resolved [DA] versus time recording with transients denoted by a red asterisk. Above each recording are individual voltammograms comparing transients (or baseline; red) to the electrically evoked signal (black). Below each recording is the pseudo-color

plot showing all voltammograms collected during the measurement in time. Whereas no DA transients were observed in the SAL recording, DA transients were present after ATX, RAC, and AMPH administration. Voltammograms confirm DA as the origin of these transients.

Figure 4B shows the average number of DA transients for each 5 min-epoch. One-way repeated measures ANOVA revealed a significant effect of time for Design 2a (left panel; $F_{11,33}$ = 6.03, $p < 0.0001$) and Design 2b (right panel; $F_{11,33} = 6.86$, $p < 0.0001$). Similar to the analysis of $[DA]_{max}$ above, the time series of DA transients was compiled into drug groups with a single control in Figure 4C. One-way repeated measures ANOVA with pseudo-replication revealed a significant effect of drug on DA transients for Design 2a (left panel; $F_{3,9} = 22.07$, $p = 0.0002$). Post-hoc tests revealed a significant increase in DA transients with ATX ($p = 0.0039$), RAC (p = 0.0001), and AMPH ($p < 0.0001$) compared to control. A significant effect of drug was also found for Design 2b (right panel; $F_{3,9} = 18.46$, $p = 0.0003$). Post-hoc tests revealed a significant increase in DA transients with ATX ($p < 0.0001$) and AMPH ($p < 0.0001$) but not RAC ($p = 0.1765$) compared to control and that AMPH increased DA transients compared to RAC ($p = 0.0102$). Taken together, these results suggest that ATX elicits DA transients in the ventral striatum with and without RAC.

ATX and basal DA

Figure 5A shows representative recordings demonstrating the effects of SAL, ATX, RAC, and AMPH on the change in basal (i.e., non-electrically evoked) DA levels in the ventral striatum following i.v. administration and using Design 2a. Each panel shows a raw FSCV (black) and PCR-resolved (red) [DA] versus time recording. Below each recording is the pseudo-color plot showing all voltammograms collected during the measurement in time. For the SAL trace, there appears to be minimal changes in the FSCV record and not unexpectedly, considerable overlap

with the PCA-resolved record. For ATX, RAC, and AMPH, there appears to be a steady decrease in the FSCV signal after drug injection, with more pronounced effects for RAC and AMPH and indicative of the non-DA changes in the pseudo-color plots. PCR processing produced no change in basal DA levels with ATX, but revealed increases with RAC and AMPH.

Figure 5B shows average values of Δ[DA] for each 5 min-epoch. One-way repeated measures ANOVA revealed a significant effect of time for Design 2a (left panel; $F_{11,77} = 14.03$, $p < 0.0001$) and Design 2b (right panel; $F_{11,33} = 22.7$, $p = 0.0115$). Per the analysis of $[DA]_{max}$ and DA transients, the time series of Δ[DA] was compiled into drug groups with a single control in Figure 5C. One-way repeated measures ANOVA with pseudo-replication revealed a significant effect of drug on Δ[DA] for Design 2a (left panel; $F_{3,9} = 86.59$, $p < 0.0001$) and Design 2b (left panel; $F_{3,9} = 9.03$, $p < 0.0044$). However, post-hoc tests revealed that only AMPH caused a significant increase in Δ[DA] with Design 2a (left panel; $p < 0.0001$) and Design 2b (right panel; $p = 0.0059$). Taken together, these results suggest that ATX does not alter basal DA levels in the striatum.

Discussion

The goal of the present study was to investigate the effects of the non-stimulant ADHD drug, ATX, on striatal DA signaling measured in real time using FSCV at a CFM. ATX did not alter electrically evoked phasic-like DA signals and basal DA levels, consistent with a lack of presynaptic effects on DA terminals in the ventral striatum. However, and indicative of proximal effects involving an activation of burst firing by DA neurons, ATX elicited DA transients. Collectively, these results suggest that, in addition to well-recognized actions of elevating NE and DA levels in the PFC, activation of phasic DA signaling in the ventral striatum is a potential mechanism by which ATX elicits therapeutic effects for treatment of ADHD.

ATX and electrically evoked phasic-like DA signals

Electrically evoked DA signals measured in real-time by FSCV at a CFM reflect the opposing actions of exocytotic DA release and DA uptake (Wightman et al., 1988). The electrically evoked DA responses evaluated in this study also mimic the amplitude and dynamics of naturally occurring DA transients (Robinson et al., 2008). Thus, because ATX did not alter $[DA]_{max}$ and the dynamics of these electrically evoked responses, we conclude that ATX does not presynaptically alter phasic DA signaling in the ventral striatum. In contrast, the D2 DA receptor antagonist, RAC, increased $[DA]_{max}$ and the duration of these electrically evoked phasic-like DA signals. The effects of RAC are consistent with blockade of presynaptic DA autoreceptors in the ventral striatum and the subsequent increase in DA release and decrease in DA uptake (Wu et al., 2002). Similarly, although not further increasing $[DA]_{max}$ above RAC levels significantly, AMPH also increases DA release and decreases DA uptake (Avelar et al., 2013; Covey et al., 2013; Daberkow et al., 2013).

Our results with ATX are in alignment with the high selectivity of ATX for NET and its low binding affinity to DAT (Bymaster et al., 2002). Anatomical studies have demonstrated that the ventral striatum receives noradrenergic projections from the locus coeruleus (LC) (Berridge et al., 1997), as well as from the nucleus tractus solitarius (NTS) (Delfs et al., 1998). Extracellular DA released in the ventral striatum may be non-preferentially cleared by NET similar to the PFC (Yamamoto & Novotney, 1998). However, the ventral striatum is predominantly innervated by VTA DA neurons and thus, has a greater population of DAT as compared to NET. Therefore, the relative abundance of DAT in the ventral striatum, coupled with the high selectivity of ATX for NET, is presumably the cause for negligible ATX effects on $[DA]_{max}$ and the duration of electrically evoked phasic-like DA signals recorded in the ventral striatum.

ATX and basal DA levels

Our study with FSCV at a CFM coupled to the chemometrics approach of PCR showed no significant ATX-induced changes in basal DA levels in the ventral striatum. This result concurs with previous microdialysis results, which showed no increase in dialysate DA collected in the nucleus accumbens with ATX (Bymaster et al., 2002) and other selective NET inhibitors, such as desipramine and reboxetine (Linner et al., 2001). Similar to results with electrically evoked phasic-like DA signals, the lack of effect of ATX on basal DA levels is inconsistent with a presynaptic target of DA terminals in the ventral striatum. Similar to ATX, RAC showed no significant effects on Δ[DA], while AMPH significantly increased this FSCV measure of basal DA levels. These later results are not entirely consistent with previous microdialysis studies, which have shown that both drugs elevate striatal dialysate DA (Hertel et al., 1999; Kuczenski et al., 1991). The basis for this discrepancy is not entirely clear but must be related to different analytical properties of the monitoring techniques. Microdialysis exhibits excellent chemical resolution and sensitivity, but its large probe damages adjacent tissue confounding quantitative studies (Borland et al., 2005; Watson et al., 2006). On the other hand, FSCV provides superior temporal and spatial resolution but is more limited by sensitivity and selectivity and hence, requires coupling with PCR to resolve DA from interferents (Keithley & Wightman, 2011). Recent studies in the mouse striatum have suggested basal DA levels to be approximately 100 nM (Atcherley et al., 2014). Because FSCV coupled to PCR has detected changes in basal DA in the lower nanomolar ranges (~5 to 40 nM; (Hart et al., 2014), this approach appears to be suitable for investigating the effects of ATX on basal DA levels.

ATX activates DA transients in the ventral striatum

Here we show that ATX, a selective NET blocker, elicits DA transients in the ventral striatum. Because ATX appears devoid of presynaptic effects on DA terminals in the ventral striatum, this result is consistent with an upstream action involving the activation of burst firing by DA neurons (Sombers et al., 2009). Indeed, the functional correlation between burst firing of DA neurons and the appearance of DA transients in DA terminal fields is well established through studies with behaving animals in response to rewards and reward-predicting cues (Schultz, 1998; Covey et al., 2013; Clark et al., 2010; Covey et al., 2014) and also with psychostimulants, such as cocaine and AMPH (Shi et al., 2000; Shi et al., 2004; Stuber et al., 2005; Koulchitsky et al., 2012; Daberkow et al., 2013). Previous studies have also shown other selective NET inhibitors to induce burst firing in VTA DA neurons (Shi et al., 2000; Linner et al., 2001; Friedman et al., 2008), perhaps mediated indirectly by the PFC and/or directly within the VTA (Darracq et al., 1998; Grenhoff et al., 1993; Grenhoff & Svensson, 1993). Confidence in the present ATX-induced activation of DA transients is supported by the excellent agreement between the observed lack of activation of DA transients by RAC alone in the anesthetized preparation but an increase after subsequent administration of psychostimulant, i.e., AMPH, and previous studies (Venton & Wightman, 2007; Park et al., 2010). Taken together, our results suggest that ATX, a non-stimulant, thus shares activation of phasic DA signaling with psychostimulants such as AMPH and cocaine.

Although our study does not elucidate the precise mechanism of action by which ATX elicits DA transients, there is evidence supporting a few possible explanations. By inhibiting NET, ATX elevates extracellular NE levels in the PFC, which receives dense noradrenergic input from the LC (Ferrucci et al., 2013). Increased cortical NE activates the post-synaptic α-1 adrenergic receptors and causes excitation of PFC neurons. The subsequent post-synaptic excitatory effect of

cortical glutamatergic afferents to the VTA can cause burst firing of DA neurons (Thierry et al., 1979; Sesack & Pickel, 1992; Karreman & Moghaddam, 1996; Darracq et al., 1998). Supporting this hypothesis are reports showing that stimulation of PFC neurons selectively increases burst firing in the VTA and enhances DA release in the nucleus accumbens (Murase et al., 1993; Taber et al., 1995), whereas application of glutamate receptor antagonist decreases extracellular DA levels in this ventral striatal region (Taber et al., 1995). Furthermore, the VTA receives direct noradrenergic innervation from the LC (Jones & Moore, 1977; Grenhoff et al., 1993) and other brain stem regions (Mejias-Aponte et al., 2009). Direct application of NE depolarizes ~60% of the DA neurons in the VTA (Grenhoff et al., 1995). Additionally, DA neuron firing increases in response to single-pulse stimulation of the LC and is attenuated in the presence of prazosin (Grenhoff et al., 1993; Grenhoff & Svensson, 1993). Thus, by blocking NE uptake at noradrenergic terminals, and thereby increasing extracellular levels of NE in the NET rich PFC, as well as in the VTA, ATX may be mediating an excitatory effect on the VTA DA neurons, leading to their phasic activation.

Therapeutic action of ATX in ADHD

The activation of DA transients in the ventral striatum by ATX may have important implications to its relevance as an ADHD drug within the purview of the DTD model. It is suggested that psychostimulant drugs, like AMPH (Adderall®) and MPH (Ritalin®), used to treat ADHD produce their therapeutic effects by increasing the amplitude of the DA transient elicited by the predictive cue and/or the reward during reinforcement learning (Tripp & Wickens, 2008). This enhanced transient activation would in turn improve associative learning between cue and reward, which is hampered in ADHD patients. Thus, activation of phasic DA signaling may be an additional contributing factor to the therapeutic effects of ATX in treatment of ADHD. However,

an important caveat to consider is ATX dose. The dose of ATX that we used (10 mg/kg) was selected, because it robustly elevates dialysate DA levels in the PFC but not in the dorsal striatum and nucleus accumbens (Bymaster et al. 2002). Previous reports with other selective NET inhibitors, nisoxetine (Shi et al., 2000; Shi et al., 2004) and reboxetine (Linner et al., 2001), have also used i.v. administration at similar doses to demonstrate an activation of burst firing of midbrain DA neurons. However, the dose of 10 mg/kg for ATX may not be therapeutically relevant and hence, the precise pharmacologic implications of ATX for treating ADHD needs further study, especially using awake animals due to the blunting effects of anesthesia on burst firing of DA neurons (Kelland et al., 1990; Chiodo, 1988).

Conclusion

Here we show, for the first time, that ATX, a selective NET-inhibitor, elicits DA transients in the ventral striatum. Hence, activation of phasic DA signaling may be a common property of ADHD drugs. Eliciting DA transients, which are the extracellular phasic signals important for reward processing and reinforcement learning, may be a possible additional mechanism of ATX in causing its therapeutic effects in ADHD. However, this suggestion must be confirmed by further study using therapeutic doses of ATX in freely behaving animal models.

REFERENCES

1. American Psychiatric Association (2013). *Diagnostic and statistical manual of mental disorders, 5th edition*.
2. Apicella, P., Ljungberg, T., Scarnati, E., & Schultz, W. (1991). Responses to reward in monkey dorsal and ventral striatum. *Experimental Brain Research, 85,* 491-500.
3. Arnsten, A. F. T. (2006). Stimulants: Therapeutic actions in ADHD. *Neuropsychopharmacology, 31,* 2376-2383.
4. Arnsten, A. F. T. & Pliszka, S. R. (2011). Catecholamine influences on prefrontal cortical function: Relevance to treatment of attention deficit/hyperactivity disorder and related disorders. *Pharmacology Biochemistry and Behavior, 99,* 211-216.
5. Arnsten, A. F. T. & Li, B. M. (2005). Neurobiology of Executive Functions: Catecholamine Influences on Prefrontal Cortical Functions. *Biological Psychiatry, 57,* 1377-1384.
6. Aston-Jones, G., Rajkowski, J., & Cohen, J. (2000). Locus coeruleus and regulation of behavioral flexibility and attention. *Cognition, Emotion and Autonomic Responses: the Integrative Role of the Prefrontal Cortex and Limbic Structures, 126,* 165-182.
7. Atcherley, C. W., Laude, N. D., Monroe, E. B., Wood, K. M., Hashemi, P., & Heien, M. L. (2014). Improved calibration of voltammetric sensors for studying pharmacological effects on dopamine transporter kinetics in vivo. *ACS Chemical Neuroscience, 6,* 1509-1516.
8. Avelar, A. J., Juliano, S. A., & Garris, P. A. (2013). Amphetamine augments vesicular dopamine release in the dorsal and ventral striatum through different mechanisms. *Journal of neurochemistry, 125,* 373-385.

9. Berridge, C. W., Devilbiss, D. M., Andrzejewski, M. E., Arnsten, A. F. T., Kelley, A. E., Schmeichel, B. et al. (2006). Methylphenidate preferentially increases catecholamine neurotransmission within the prefrontal cortex at low doses that enhance cognitive function. *Biological Psychiatry, 60,* 1111-1120.
10. Berridge, C. W. & Stalnaker, T. A. (2002). Relationship between low-dose amphetamine-induced arousal and extracellular norepinephrine and dopamine levels within prefrontal cortex. *Synapse, 46,* 140-149.
11. Berridge, C. W. & Stalnaker, T. A. (2002). Relationship between low-dose amphetamine-induced arousal and extracellular norepinephrine and dopamine levels within prefrontal cortex. *Synapse, 46,* 140-149.
12. Berridge, C. W., Stratford, T. L., Foote, S. L., & Kelley, A. E. (1997). Distribution of dopamine b-hydroxylase-like immunoreactive fibers within the shell subregion of the nucleus accumbens. *SYNAPSE-NEW YORK-, 27,* 230-241.
13. Berridge, K. C. (2001). Reward learning: Reinforcement, incentives, and expectations. *Psychology of Learning and Motivation: Advances in Research and Theory, Vol 40, 40,* 223-278.
14. Borland, L. M., Shi, G., Yang, H., & Michael, A. C. (2005). Voltammetric study of extracellular dopamine near microdialysis probes acutely implanted in the striatum of the anesthetized rat. *Journal of Neuroscience Methods, 146,* 149-158.
15. Bymaster, F. P., Katner, J. S., Nelson, D. L., Hemrick-Luecke, S. K., Threlkeld, P. G., Heiligenstein, J. H. et al. (2002). Atomoxetine increases extracellular levels of norepinephrine and dopamine in prefrontal cortex of rat: A potential mechanism for efficacy in Attention Deficit/Hyperactivity Disorder. *Neuropsychopharmacology, 27,* 699-711.

16. Bymaster, F. P., Katner, J. S., Nelson, D. L., Hemrick-Luecke, S. K., Threlkeld, P. G., Heiligenstein, J. H. et al. (2002). Atomoxetine Increases Extracellular Levels of Norepinephrine and Dopamine in Prefrontal Cortex of Rat: A Potential Mechanism for Efficacy in Attention Deficit/Hyperactivity Disorder. *Neuropsychopharmacology, 27,* 699-711.
17. Castellanos, F. X., Giedd, J. N., Marsh, W. L., Hamburger, S. D., Vaituzis, A. C., Dickstein, D. P. et al. (1996). Quantitative brain magnetic resonance imaging in attention-deficit hyperactivity disorder. *Archives of General Psychiatry, 53,* 607-616.
18. Castellanos, F. X. & Tannock, R. (2002). Neuroscience of attention-deficit/hyperactivity disorder: the search for endophenotypes. *Nat Rev Neurosci, 3,* 617-628.
19. Chiodo, L. A. (1988). Dopamine-containing neurons in the mammalian central nervous system: electrophysiology and pharmacology. *Neuroscience & Biobehavioral Reviews, 12,* 49-91.
20. Clark, J. J., Sandberg, S. G., Wanat, M. J., Gan, J. O., Horne, E. A., Hart, A. S. et al. (2010). Chronic microsensors for longitudinal, subsecond dopamine detection in behaving animals. *Nature methods, 7,* 126-129.
21. Covey, D. P., Juliano, S. A., & Garris, P. A. (2013). Amphetamine Elicits Opposing Actions on Readily Releasable and Reserve Pools for Dopamine. *Plos One, 8*.
22. Covey, D. P., Roitman, M. F., & Garris, P. A. (2014). Illicit dopamine transients: reconciling actions of abused drugs. *Trends in neurosciences, 37,* 200-210.
23. Daberkow, D. P., Brown, H. D., Bunner, K. D., Kraniotis, S. A., Doellman, M. A., Ragozzino, M. E. et al. (2013). Amphetamine Paradoxically Augments Exocytotic Dopamine Release and Phasic Dopamine Signals. *Journal of Neuroscience, 33,* 452-463.

24. Darracq, L., Blanc, G., Glowinski, J., & Tassin, J. P. (1998). Importance of the noradrenaline-dopamine coupling in the locomotor activating effects of D-amphetamine. *Journal of Neuroscience, 18,* 2729-2739.

25. Delfs, J. M., Zhu, Y., Druhan, J. P., & Aston-Jones, G. S. (1998). Origin of noradrenergic afferents to the shell subregion of the nucleus accumbens: anterograde and retrograde tract-tracing studies in the rat. *Brain research, 806,* 127-140.

26. Ferrucci, M., Giorgi, S., Bartalucci, A., Busceti, L., & Fornai, F. (2013). The effects of locus coeruleus and norepinephrine in methamphetamine toxicity. *Current neuropharmacology, 11,* 80-94.

27. Friedman, A., Friedman, Y., Dremencov, E., & Yadid, G. (2008). VTA dopamine neuron bursting is altered in an animal model of depression and corrected by desipramine. *Journal of Molecular Neuroscience, 34,* 201-209.

28. Grenhoff, J., Nisell, M., Ferr+¬, S., Aston-Jones, G., & Svensson, T. H. (1993). Noradrenergic modulation of midbrain dopamine cell firing elicited by stimulation of the locus coeruleus in the rat. *J.Neural Transmission, 93,* 11-25.

29. Grenhoff, J., Nisell, M., Ferre, S., Astonjones, G., & Svensson, T. H. (1993). Noradrenergic Modulation of Midbrain Dopamine Cell Firing Elicited by Stimulation of the Locus-Ceruleus in the Rat. *Journal of Neural Transmission-General Section, 93,* 11-25.

30. Grenhoff, J. & Svensson, T. H. (1993). Prazosin Modulates the Firing Pattern of Dopamine Neurons in Rat Ventral Tegmental Area. *European Journal of Pharmacology, 233,* 79-84.

31. Grenhoff, J., North, R. A., & Johnson, S. W. (1995). Alpha1GÇÉadrenergic Effects on Dopamine Neurons Recorded Intracellularly in the Rat Midbrain Slice. *European Journal of Neuroscience, 7,* 1707-1713.

32. Hart, A. S., Rutledge, R. B., Glimcher, P. W., & Phillips, P. E. (2014). Phasic dopamine release in the rat nucleus accumbens symmetrically encodes a reward prediction error term. *The Journal of neuroscience, 34,* 698-704.

33. Heien, M. L. A. V., Johnson, M. A., & Wightman, R. M. (2004). Resolving Neurotransmitters Detected by Fast-Scan Cyclic Voltammetry. *Analytical Chemistry, 76,* 5697-5704.

34. Hertel, P., Fagerquist, M. V., & Svensson, T. H. (1999). Enhanced cortical dopamine output and antipsychotic-like effects of raclopride by +¦2 adrenoceptor blockade. *Science, 286,* 105-107.

35. Jones, B. E. & Moore, R. Y. (1977). Ascending projections of the locus coeruleus in the rat. II. Autoradiographic study. *Brain research, 127,* 23-53.

36. Karreman, M. & Moghaddam, B. (1996). The prefrontal cortex regulates the basal release of dopamine in the limbic striatum: an effect mediated by ventral tegmental area. *Journal of neurochemistry, 66,* 589-598.

37. Kawagoe, R., Takikawa, Y., & Hikosaka, O. (1998). Expectation of reward modulates cognitive signals in the basal ganglia. *Nature neuroscience, 1,* 411-416.

38. Keithley, R. B. & Wightman, R. M. (2011). Assessing principal component regression prediction of neurochemicals detected with fast-scan cyclic voltammetry. *ACS chemical neuroscience, 2,* 514-525.

39. Kelland, M. D., Chiodo, L. A., & Freeman, A. S. (1990). Anesthetic influences on the basal acticity and pharmacological responsiveness of nigrostriatal dopamine neurons. *Synapse, 6,* 207-209.

40. Koulchitsky, S., De Backer, B., Quertemont, E., Charlier, C., & Seutin, V. (2012). Differential effects of cocaine on dopamine neuron firing in awake and anesthetized rats. *Neuropsychopharmacology, 37,* 1559-1571.

41. Kuczenski, R. & Segal, D. S. (2001). Locomotor effects of acute and repeated threshold doses of amphetamine and methylphenidate: Relative roles of dopamine and norepinephrine. *Journal of Pharmacology and Experimental Therapeutics, 296,* 876-883.
42. Kuczenski, R., Segal, D. S., & Aizenstein, M. L. (1991). Amphetamine, cocaine, and fencamfamine: relationship between locomotor and stereotypy response profiles and caudate and accumbens dopamine dynamics. *The Journal of neuroscience, 11,* 2703-2712.
43. Kume-Kick, J. & Rice, M. E. (1998). Dependence of dopamine calibration factors on media Ca 2+ and Mg 2+ at carbon-fiber microelectrodes used with fast-scan cyclic voltammetry. *Journal of neuroscience methods, 84,* 55-62.
44. Levy, F. (2009). Dopamine vs noradrenaline: inverted-U effects and ADHD theories. *Australian and New Zealand Journal of Psychiatry, 43,* 101-108.
45. Linner, L., Endersz, H., Ohman, D., Bengtsson, F., Schalling, M., & Svensson, T. H. (2001). Reboxetine modulates the firing pattern of dopamine cells in the ventral tegmental area and selectively increases dopamine availability in the prefrontal cortex. *Journal of Pharmacology and Experimental Therapeutics, 297,* 540-546.
46. Lou, H. C., Henriksen, L., Bruhn, P., Borner, H., & Nielsen, J. B. (1989). Striatal Dysfunction in Attention Deficit and Hyperkinetic Disorder. *Archives of Neurology, 46,* 48-52.
47. Mejias-Aponte, C. A., Drouin, C., & Aston-Jones, G. (2009). Adrenergic and noradrenergic innervation of the midbrain ventral tegmental area and retrorubral field: prominent inputs from medullary homeostatic centers. *The Journal of neuroscience, 29,* 3613-3626.
48. Michael, D., Travis, E. R., & Wightman, R. M. (1998). Peer reviewed: color images for fast-scan CV measurements in biological systems. *Analytical chemistry, 70,* 586A-592A.

49. Murase, S., Grenhoff, J., Chouvet, G., Gonon, F. G., & Svensson, T. H. (1993). Prefrontal cortex regulates burst firing and transmitter release in rat mesolimbic dopamine neurons studied in vivo. *Neuroscience letters, 157,* 53-56.

50. Park, J., Aragona, B. J., Kile, B. M., Carelli, R. M., & Wightman, R. M. (2010). In vivo voltammetric monitoring of catecholamine release in subterritories of the nucleus accumbens shell. *Neuroscience, 169,* 132-142.

51. Paxinos, G. & Watson, C. (2007). *The Rat Brain in Stereotaxic Coordinates: Hard Cover Edition*. Elsevier Science.

52. Ramsson, E. S., Covey, D. P., Daberkow, D. P., Litherland, M. T., Juliano, S. A., & Garris, P. A. (2011). Amphetamine Augments Action Potential-Dependent Dopaminergic Signaling in the Striatum in Vivo. *Journal of neurochemistry, 117,* 937-948.

53. Roberts, J., Lugo-Morales, L., Loziuk, P., & Sombers, L. (2013). Real-Time Chemical Measurements of Dopamine Release in the Brain. In N.Kabbani (Ed.), *Dopamine* (964 ed., pp. 275-294). Humana Press.

54. Roberts, J., Lugo-Morales, L., Loziuk, P., & Sombers, L. (2013). Real-Time Chemical Measurements of Dopamine Release in the Brain. In N.Kabbani (Ed.), *Dopamine* (964 ed., pp. 275-294). Humana Press.

55. Robinson, D. L., Venton, B. J., Heien, M. L. A. V., & Wightman, R. M. (2003). Detecting subsecond dopamine release with fast-scan cyclic voltammetry in vivo. *Clinical Chemistry, 49,* 1763-1773.

56. Robinson, D. L., Hermans, A., Seipel, A. T., & Wightman, R. M. (2008). Monitoring rapid chemical communication in the brain. *Chemical reviews, 108,* 2554-2584.

57. Schultz, W. (1998). Predictive reward signal of dopamine neurons. *Journal of Neurophysiology, 80,* 1-27.

58. Schultz, W. (1998). Predictive reward signal of dopamine neurons. *Journal of Neurophysiology, 80,* 1-27.

59. Sesack, S. R. & Pickel, V. M. (1992). Prefrontal cortical efferents in the rat synapse on unlabeled neuronal targets of catecholamine terminals in the nucleus accumbens septi and on dopamine neurons in the ventral tegmental area. *Journal of Comparative Neurology, 320,* 145-160.

60. Shi, W. X., Pun, C. L., Zhang, X. X., Jones, M. D., & Bunney, B. S. (2000). Dual effects of D-amphetamine on dopamine neurons mediated by dopamine and nondopamine receptors. *Journal of Neuroscience, 20,* 3504-3511.

61. Shi, W. X., Pun, C. L., & Zhou, Y. (2004). Psychostimulants induce low-frequency oscillations in the firing activity of dopamine neurons. *Neuropsychopharmacology, 29,* 2160-2167.

62. Shi, W. X., Pun, C. L., & Zhou, Y. (2004). Psychostimulants Induce Low-Frequency Oscillations in the Firing Activity of Dopamine Neurons. *Neuropsychopharmacology, 29,* 2160-2167.

63. Sombers, L. A., Beyene, M., Carelli, R. M., & Wightman, R. M. (2009). Synaptic overflow of dopamine in the nucleus accumbens arises from neuronal activity in the ventral tegmental area. *The Journal of neuroscience, 29,* 1735-1742.

64. Stuber, G. D., Wightman, R. M., & Carelli, R. M. (2005). Extinction of cocaine self-administration reveals functionally and temporally distinct dopaminergic signals in the nucleus accumbens. *Neuron, 46,* 661-669.

65. Taber, M. T., Das, S., & Fibiger, H. C. (1995). Cortical regulation of subcortical dopamine release: mediation via the ventral tegmental area. *Journal of neurochemistry, 65,* 1407-1410.

66. Thierry, A. M., Deniau, J. M., & Feger, J. (1979). Effects of stimulation of the frontal cortex on identified output VMT cells in the rat. *Neuroscience letters, 15,* 103-107.

67. Tripp, G. & Wickens, J. R. (2008). Research Review: Dopamine transfer deficit: a neurobiological theory of altered reinforcement mechanisms in ADHD. *Journal of Child Psychology and Psychiatry, 49,* 691-704.

68. Venton, B. J. & Wightman, R. M. (2007). Pharmacologically induced, subsecond dopamine transients in the caudateGÇôputamen of the anesthetized rat. *Synapse, 61,* 37-39.

69. Wightman, R. M., Amatorh, C., Engstrom, R. C., Hale, P. D., Kristensen, E. W., Kuhr, W. G. et al. (1988). Real-time characterization of dopamine overflow and uptake in the rat striatum. *Neuroscience, 25,* 513-523.

70. Wightman, R. M., Heien, M. L. A. V., Wassum, K. M., Sombers, L. A., Aragona, B. J., Khan, A. S. et al. (2007). Dopamine release is heterogeneous within microenvironments of the rat nucleus accumbens. *European Journal of Neuroscience, 26,* 2046-2054.

71. Woodard, G. E. O. F. (1965). Principles in drug administration. *Methods of animal experimentation, 1,* 343-359.

72. Wu, Q., Reith, M. E., Wightman, R. M., Kawagoe, K. T., & Garris, P. A. (2001). Determination of release and uptake parameters from electrically evoked dopamine dynamics measured by real-time voltammetry. *Journal of neuroscience methods, 112,* 119-133.

73. Wu, Q., Reith, M. E., Walker, Q. D., Kuhn, C. M., Carroll, F. I., & Garris, P. A. (2002). Concurrent autoreceptor-mediated control of dopamine release and uptake during neurotransmission: an in vivo voltammetric study. *The Journal of neuroscience, 22,* 6272-6281.

74. Yamamoto, B. K. & Novotney, S. (1998). Regulation of extracellular dopamine by the norepinephrine transporter. *Journal of neurochemistry, 71,* 274-280.

CHAPTER I FIGURES

Figure 1

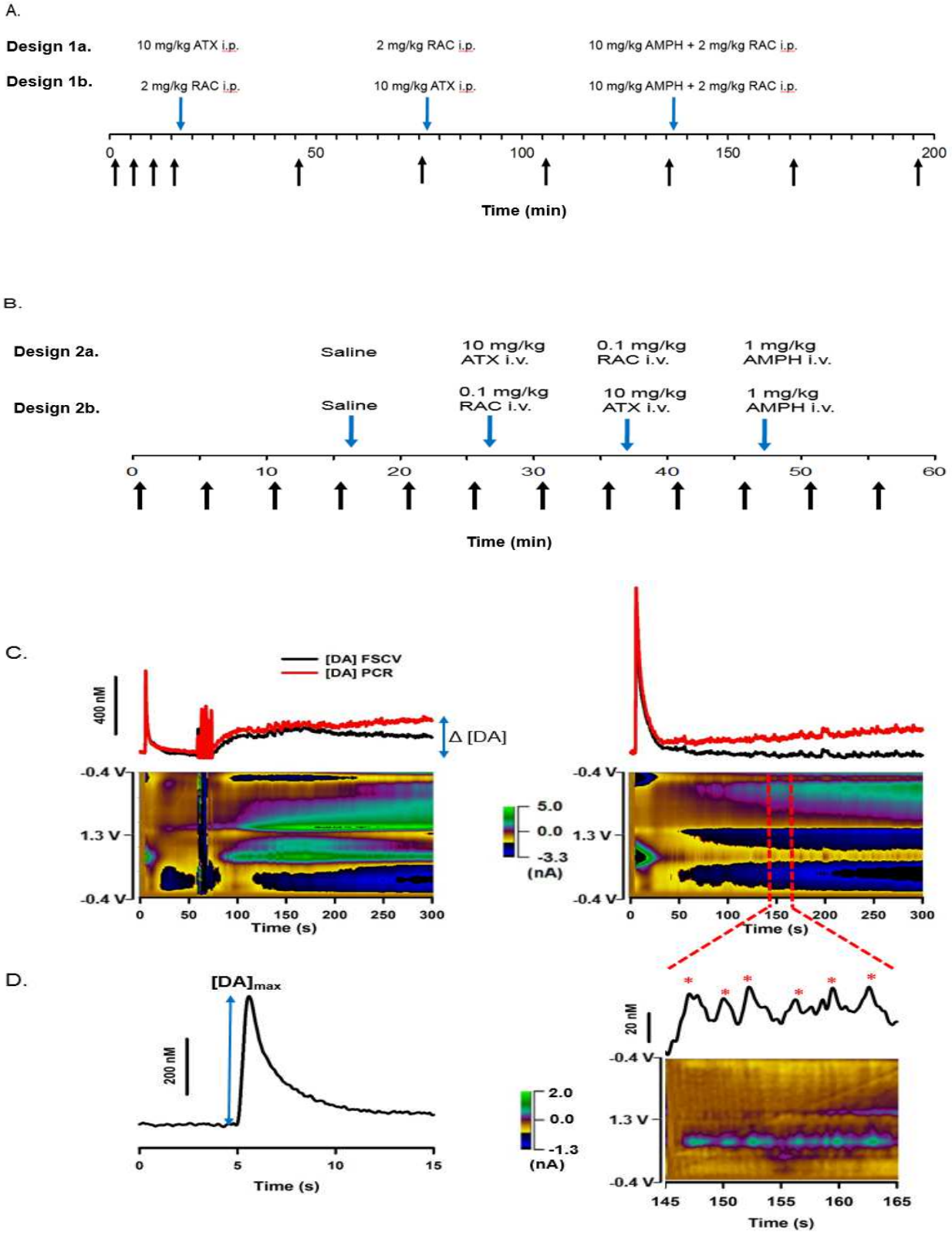

Figure 1. *Experimental design and data analysis.* A) Experimental Design 1 for i.p. drug administration. Electrical stimulation is indicated by black arrows; drug injection is indicated by blue arrows. Design 1a: Three pre-drug electrically evoked signals were collected, followed by administration of ATX. After collecting a 60-min post-ATX trace, RAC was injected. Collection of the 60-min post-RAC trace was follwed by administration of the positive control, AMPH, co-administered with a second dose of RAC. Design 1b: Similar to Design 1a, except that the order of administration of RAC and ATX was reversed. B) Experimental Design 2 for i.v. drug administration. Electrical stimulation is indicated by black arrows; drug injection is indicated by blue arrows. Design 2a: Three pre-drug electrically evoked signals were collected, followed by administration of SAL, which was the negative control. ATX was injected after the 10-min post-SAL trace, followed by admistration of RAC and AMPH (positive control). Design 2b: Similar to Design 2a, except that the order of administration of RAC and ATX was reversed. C) (Top) FSCV (black line) and PCR (red line) traces for exemplar recordings pre- (left) and post- (right) AMPH. (Bottom) Pseudo-color plots for both representative recordings showing multiple analytes in the non-electrically evoked portion. The PCR resolved trace was used to analyze changes in basal DA (Δ[DA]). Below is a 20-s representative recording showing DA transients in the non-electrically evoked portion of the 5-min post-AMPH epoch. The PCR-resolved DA trace was used to analayze DA transients. (INSET, Top) DA transients on the PCR trace are denoted by red asterisks. (INSET, Bottom) Pseudo-color plot confirms identity of the analyte as DA. D) An exemplar electrically evoked DA signal determined from the raw FSCV signal was used to determine the maximal amplitude of the electrically evoked DA signal ($[DA]_{max}$).

Figure 2

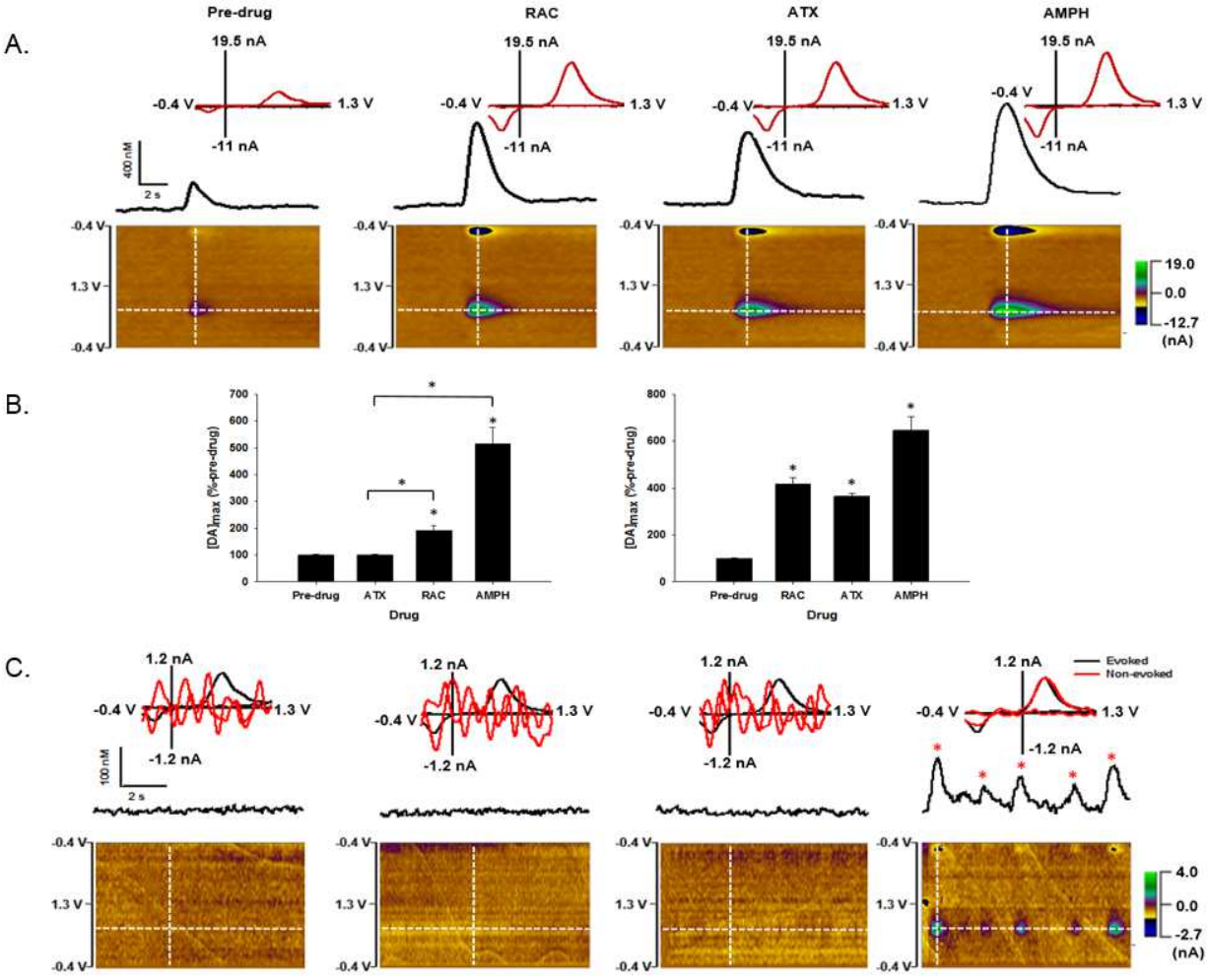

Figure 2. *Effects of ATX, RAC, and AMPH (i.p) on electrically evoked phasic-like DA signals.* A) (Top) DA signals elicited by electrical stimulation: pre-drug, post-RAC, post ATX, and post-AMPH (left to right). INSET. Individual voltammograms taken from the peak signal (white vertical line on the pseudo-color plot) identify the analyte as DA. (Bottom) Pseudo-color plots of electrically evoked DA signals collected pre-drug, post-RAC, post-ATX, and post-AMPH (left to right). White horizontal line on the pseudo-color plot identifies the DA peak oxidative potential where the evoked DA trace was collected. B) average $[DA]_{max.}$ One-way repeated measures ANOVA revealed a significant effect of drug on $[DA]_{max}$ in Design 1a (left panel) and 1b (right panel). Data are expressed as a percent of pre-drug and are mean ±SEM.*, $p < 0.05$. C) Effects of ATX, RAC, and AMPH (i.p) on DA transients. Representative pseudo-color plots of the non-electrically evoked portion of pre-drug, RAC, ATX, and AMPH recordings (left to right). **INSET.** Normalized voltammograms taken from the electrically-evoked response (black line) and a DA transient or baseline (red line) collected at the white vertical line in the pseudo-color plot.

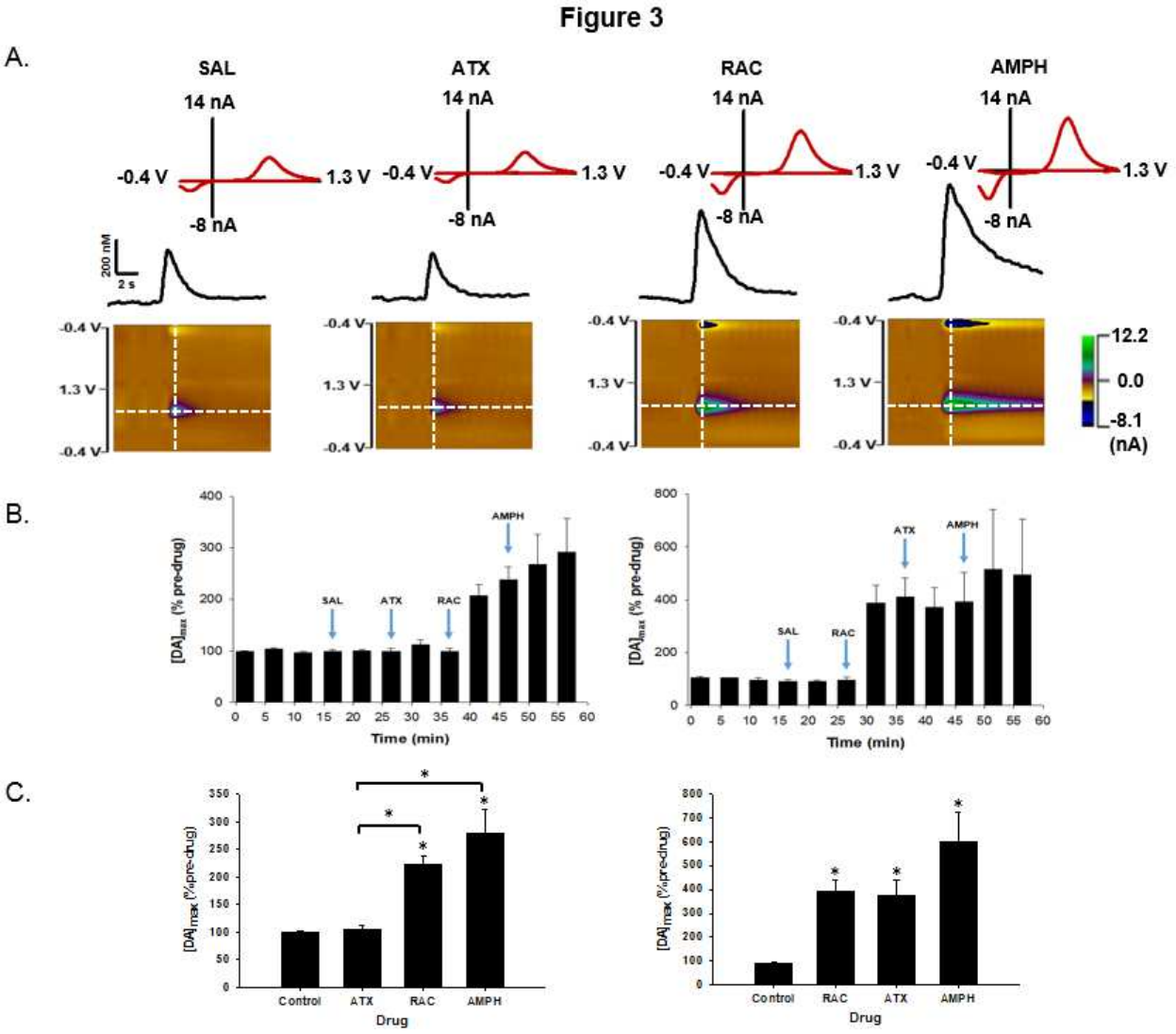

Figure 3. *Effects of SAL, ATX, RAC, and AMPH on electrically evoked phasic-like DA signals.* A) (Top) DA signals elicited by electrical stimulation: SAL, ATX, RAC, and AMPH (left to right). INSET. Individual voltammograms taken from the peak signal (white vertical line in the pseudo-color plot) identify the analyte as DA. (Bottom) Pseudo-color plots of electrically evoked DA signals SAL, ATX, RAC, and AMPH (left to right). White horizontal line in the pseudo-color plot identifies the DA peak oxidative potential where the evoked DA trace was collected. B) One-way repeated measures ANOVA revealed a significant effect of time on $[DA]_{max}$ in Design 2a (left panel) and 2b (right panel). Data are expressed as a percent of pre-drug and are mean ±SEM. C) One-way repeated measures ANOVA revealed a significant effect of drug on $[DA]_{max}$ in Design 2a (left panel) and 2b (right panel). Data are expressed as a percent of pre-drug and are mean ±SEM.*, $p < 0.05$.

Figure 4

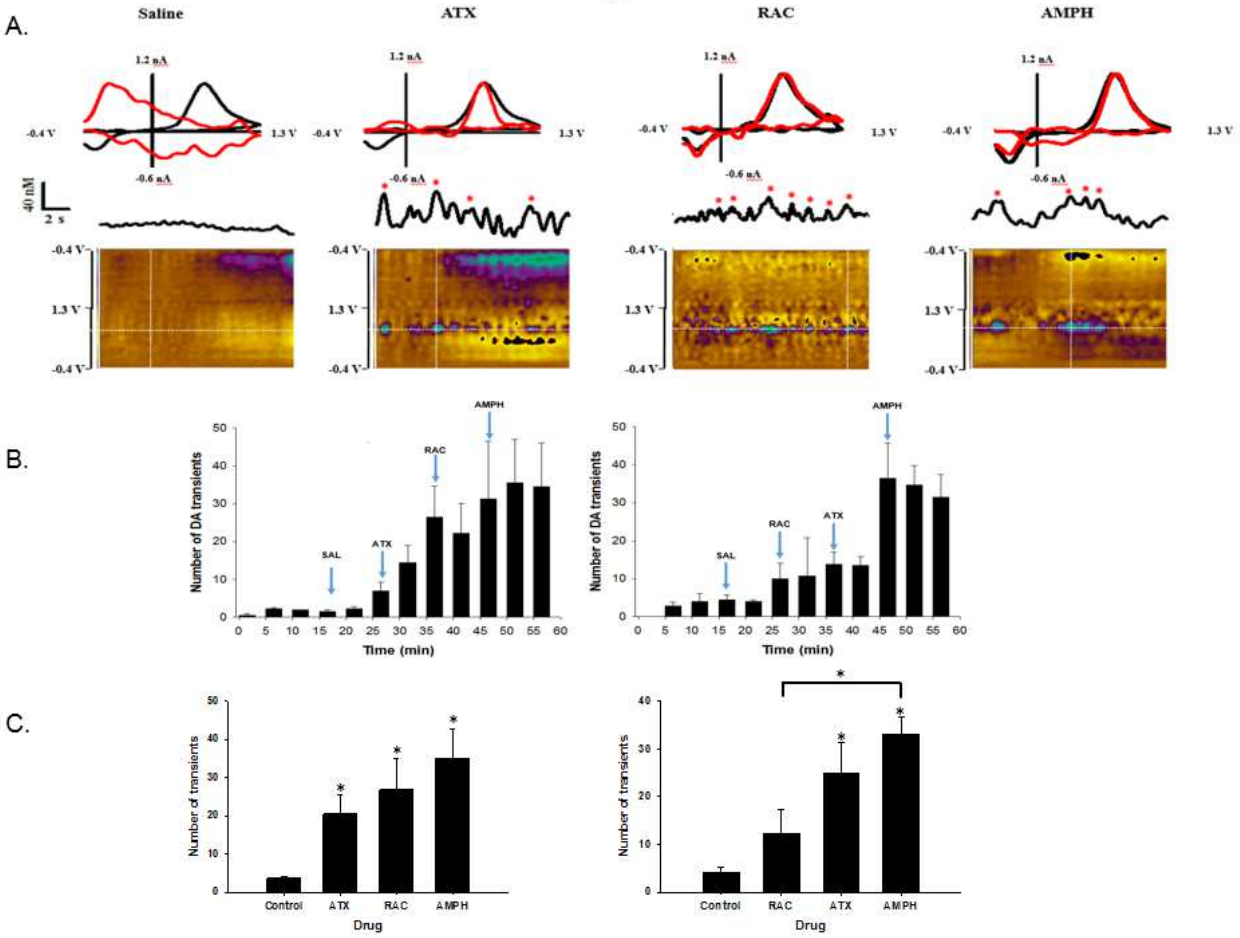

Figure 4. *Effects of SAL, ATX, RAC, and AMPH on DA transients.* A) Representative recordings of DA transients in the ventral striatum. (Top) Normalized voltammograms taken from the electrically-evoked response (black line) and a DA transient or baseline (red line) collected at the white vertical line in the pseudo-color plot. (Middle) DA transients (denoted by red asterisks) are displayed in the PCR-resolved DA trace. (Bottom) A pseudo-color plot underneath serially displays all voltammograms in time. **B)** One-way repeated measures ANOVA showed a significant effect of time on the number of DA transients in Design 2a (left panel) and 2b (right panel). Data are mean ±SEM. C) One-way repeated measures ANOVA showed a significant effect of drug on the number of DA transients in Design 2a (left panel) and 2b (right panel). Data are mean ±SEM.*, $p < 0.05$.

Figure 5

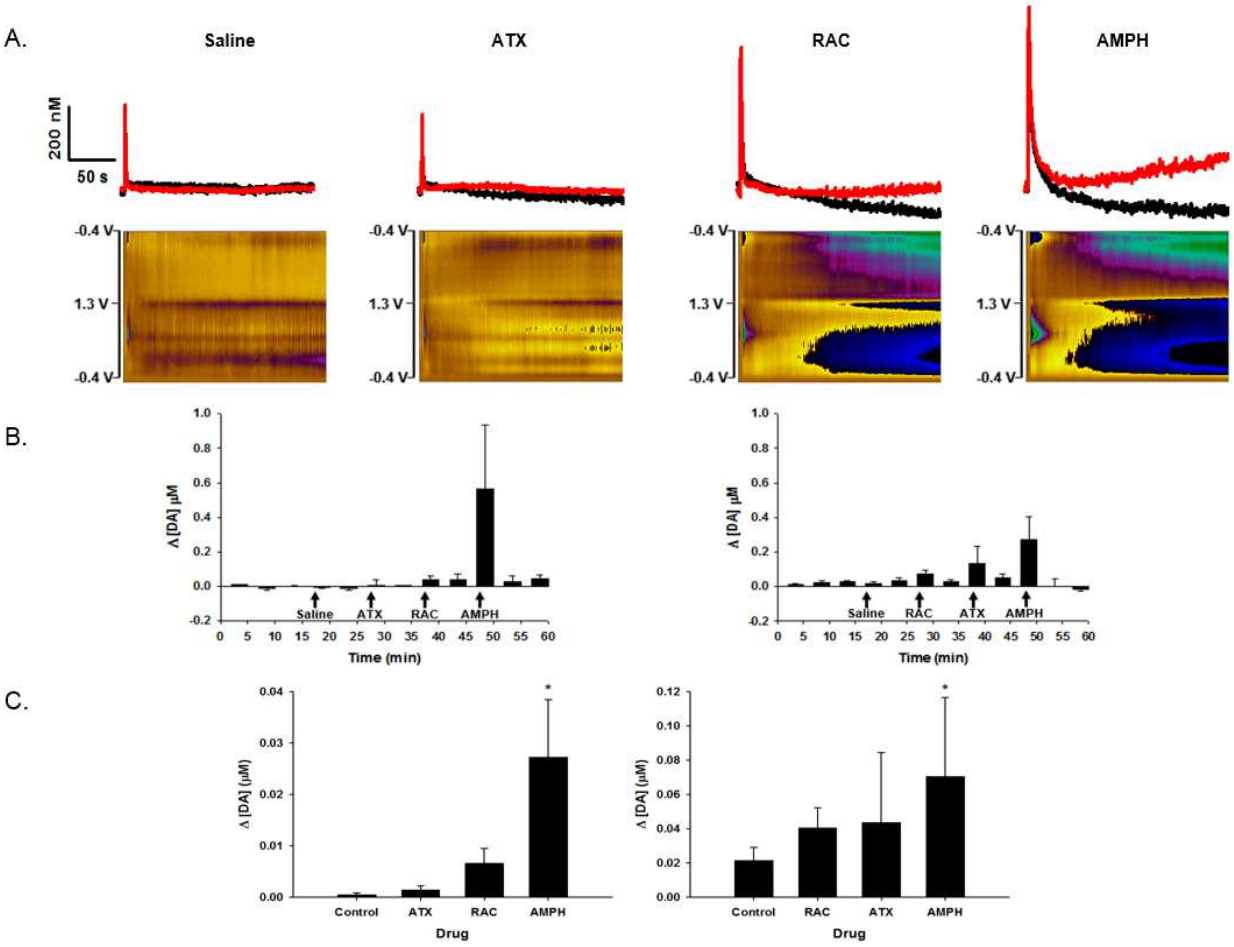

Figure 5. *Effects of ATX, RAC, and AMPH on changes in basal DA in the ventral striatum.* A) (Top) FSCV (black line) and PCR (red line) traces for exemplar recordings: SAL, ATX, RAC, and AMPH (left to right). (Bottom) Pseudo-color plots for representative recordings showing multiple analytes in the non-electrically evoked portion. The PCR resolved trace was used to analyze changes in basal DA. B) One-way repeated measures ANOVA showed a significant effect of time on Δ[DA] in Design 2a (left panel) and 2b (right panel). Data are mean ±SEM. C) One-way repeated measures ANOVA showed a significant effect of drug on Δ[DA] in Design 2a (left panel) and 2b (right panel). Data are mean ± SEM. *, $p < 0.05$.

CHAPTER II

DOPAMINE TRANSPORTER-INHIBITING PSYCHOSTIMULANTS INCREASE EXOCYTOTIC DOPAMINE RELEASE

ABSTRACT

There is increasing evidence suggesting that psychostimulants elevate brain extracellular dopamine not only by inhibiting dopamine uptake but also by increasing exocytotic dopamine release. Psychostimulant-induced increases in exocytotic dopamine release have been demonstrated by fitting electrically evoked dopamine signals measured using fast-scan cyclic voltammetry at a carbon-fiber microelectrode to the diffusion gap model, which describes dopamine diffusing across a gap between release and uptake sites and measurement at the microsensor. However, this model fails to describe features regularly observed in evoked dopamine signals, such as "hang-up", the slow return of dopamine to baseline, and incongruous changes in "lag", the time for dopamine to increase after stimulus initiation, and "overshoot", the continued dopamine increase after stimulus cessation. The recently proposed restricted diffusion model addresses these issues by dividing extracellular space into inner and outer compartments. Dopamine is initially released into the inner compartment and is transported by restricted diffusion to the outer compartment, where it is measured by the microsensor and cleared by dopamine uptake. Hang-up, attributed to dopamine adsorption to the microsensor, is removed from data prior to analysis. Here we analyze the *in vivo* effects of the psychostimulants, amphetamine, cocaine, and modafinil, on exocytotic dopamine release and dopamine uptake. Parameters describing these mechanisms and previously determined with the diffusion gap model were compared to those obtained by the restricted diffusion model. Both models similarly demonstrated an increase in exocytotic dopamine release and inhibition of dopamine uptake for all three psychostimulants.

These results support the hypothesis that psychostimulants elevate extracellular dopamine by targeting both exocytotic dopamine release and dopamine uptake.

INTRODUCTION

The mechanism of psychostimulant action has been the subject of intense scrutiny over the years. These drugs cause their behavioral effects, at least in part, by elevating extracellular DA in the dorsal and ventral striatum (Carboni et al., 1989; Di Chiara & Imperato, 1988; Carboni et al., 1989). A well-established action of one class of psychostimulants is inhibition of the dopamine transporter (DAT), which regulates extracellular DA levels by clearing released DA. Based on their interactions with DAT on DA terminals, psychostimulants have been classified as being cocaine-like or amphetamine (AMPH)-like. Cocaine-like drugs are traditional inhibitors of DAT, whereas AMPH-like drugs are DAT "substrates" (Seiden et al., 1993). AMPH-like psychostimulants are also referred to as "releasers", due to their property of eliciting reverse transport by DAT thereby causing non-action potential-dependent DA efflux (Sulzer et al., 1995). While both cocaine-like and AMPH-like drugs share the mechanism of competitive inhibition of DA uptake, these psychostimulants have been thought to differ in their actions on vesicular pools of DA and exocytotic DA release. Whereas cocaine has been shown to augment exocytotic DA release (Jones et al., 1995; Venton et al., 2006), AMPH depletes vesicular DA pools and hence, compromises exocytotic DA release (Jones et al., 1998; Schmitz et al., 2001). Therefore, DAT inhibition and DA efflux driven by translocation of DA from vesicular to cytosolic pools have been considered to be the predominant effects of AMPH action contributing to its elevation of extracellular levels of striatal DA (Sulzer, 2011; Fleckenstein et al., 2007). Evidence from some psychostimulant studies are in support of the hypothesis that in addition to blocking DA uptake, psychostimulants also increase exocytotic DA release. These studies report increased exocytotic

DA release with methylphenidate (MPH) and other DAT blockers, such as nomifensine (Venton et al., 2006; Chadchankar et al., 2012; Lee et al., 2001), in addition to cocaine (Jones et al., 1995; Venton et al., 2006). However, AMPH enhancing exocytotic DA release still remains a controversial idea due to discrepant results obtained from *in vitro* (Jones et al., 1998; Schmitz et al., 2001) and *in vivo* studies (Daberkow et al., 2013; Ramsson et al., 2011).

Kinetic analysis of electrically evoked DA signals measured by fast scan cyclic voltammetry (FSCV) at a carbon fiber microelectrode (CFM) has been used to assess the action of psychostimulants on DA release and uptake. The Wightman model, also known as the diffusion gap (DG) model, has been typically used. The DG model describes extracellular DA concentration as a balance between the opposing actions of DA release and uptake (Wightman et al., 1988). The DA measurement with FSCV is also subject to the diffusional distortions, lag (i.e., the delay in rise of the DA signal with stimulus onset) and overshoot (i.e., the continued rise of DA signal after stimulus cessation), arising from the presence of a gap between DA release and uptake sites on terminals and the CFM (Wightman et al., 1988; Kawagoe et al., 1992) (Fig. 1a). Using the DG model, we have previously reported that the psychostimulants, modafinil (MOD), AMPH, and cocaine, not only inhibit DA uptake but also increase action potential-dependent, vesicular DA release (Ramsson et al., 2011; Daberkow et al., 2013; Covey et al., 2013; Bobak et al., 2016). However, demonstrated insufficiencies in the DG model have challenged its appropriateness and hence, the finding of enhanced DA release with psychostimulants. For example, the DG model does not hold true for DA signals that show lag without overshoot or overshoot without lag (Moquin & Michael, 2009; Walters et al., 2014). The concept of a diffusion gap also fails to explain another feature regularly observed in DA signals, called hang-up or the prolonged elevation of the signal and its delayed return to baseline (Walters et al., 2014).

A new kinetic model, called the restricted diffusion (RD) model, has been recently developed (Walters et al., 2015; Walters et al., 2014) to address limitations with the DG model. The RD model (Fig. 1b) divides brain extracellular space into inner and outer compartments, with DA released into the inner compartment and transported by restricted diffusion to the outer compartment where it is detected by the CFM and cleared by uptake. The restricted diffusion of DA from the inner to outer compartment could be due to several factors, such as pockets of extracellular dead space, DA binding sites, and tissue tortuosity (Sykova & Nicholson, 2008). The model convincingly explains lag as a consequence of DA being held up, or restricted, as it diffuses to the outer compartment after release, and overshoot as the delayed arrival of DA to the CFM after overcoming the diffusional restrictions in its path. Through this concept of delayed DA transport from the release site to the CFM, the RD model also effectively provides plausible scenarios for the fast and slow-type responses recorded in the rat dorsal striatum, which are not always amenable to description by the DG model (Taylor et al., 2013; Walters et al., 2014). Additionally, hang-up has been attributed to adsorption of DA to the CFM surface and can be corrected using an equation expressing the hang-up component as a balance between the concentration of DA adsorbed and desorbed (Walters et al., 2015). Hence, the RD model improves the kinetic analysis of electrically evoked DA signals to resolve the presynaptic mechanisms of DA release and uptake.

The purpose of this study was to compare the analysis of psychostimulant effects on electrically evoked DA signals measured by FSCV at a CFM using the DG and RD models. Specifically, we used the RD model to re-analyze already published electrically evoked DA signals altered by MOD, AMPH, and cocaine and evaluated by the DG model. Our results support

the hypothesis that the DAT-inhibiting psychostimulants, AMPH, cocaine, and MOD, also augment action potential-dependent, exocytotic DA release.

RESULTS AND DISCUSSION

Correction of raw FSCV signals

As described in Figure 2, correction for the hang-up component was required for most electrically evoked DA signals kinetically analyzed by the RD model. The pseudo-color plot (Fig. 2A) suggests that the raw FSCV signal (black line), representing the electrically evoked signal (Fig. 2B) and measured at the peak oxidation potential for DA (indicated by horizontal white line on the pseudo-color plot), originates from DA. The individual voltammogram (Fig. 2A inset), determined at the peak of the evoked signal (indicated by the vertical white line on the pseudo-color plot), is also consistent with DA. This raw FSCV trace shows the hang-up component (i.e. it does not return quickly to baseline), because DA uptake would lower extracellular DA faster. To correct for hang-up, this component was first calculated using Eq. 4, which uses first-order rate constants to describe hang-up as a balance between DA adsorption to and desorption from the CFM surface. The calculated hang-up component (Fig. 2B; gray line) was then subtracted from the raw response measured by FSCV (black line) to generate a corrected signal (red line). It is noteworthy that previous uses of the DG model described herein did not involve any hang-up correction. However, the signals that were analyzed using this model were routinely cut off in time to avoid distortion by the hang-up component.

When present, the effect of pH on the raw FSCV signal, usually an alkaline shift due to changes in blood flow elicited by the same electrical stimulation evoking DA release in urethane-anesthetized animals (Robinson et al., 2003; Venton et al., 2003), was removed using the differential correction method (Venton et al., 2003). As can be seen in pseudo-color plot of Figure

3A, electrical stimulation elicits electrochemical features other than DA, the most prominent of which is pH. As shown in Figure 3B, the raw electrically evoked FSCV signal (black line) is distorted by this pH signal, which is highlighted by a considerable drop below baseline. The identity of the analytes elicited by electrical stimulation is perhaps more clearly demonstrated by their respective individual voltammograms. For example, the initial signal elicited by electrical stimulation is indicative of DA (Fig. 3A inset, left; voltammogram determined by the first vertical white line). Slower changes in the record were confirmed as pH (Fig. 3A inset, right; voltammogram determined by the second vertical white line). To correct for pH, its voltammogram was determined a few seconds after stimulation and in the absence of any DA release and used to calculate a pH signal (Fig. 3B; blue line). This signal, after adjusting to correspond to the DA oxidative potential, was then subtracted from the raw FSCV to calculate a pH-corrected DA signal (Fig. 3B; red line). This correction has also been applied previously to evoked DA signals subject to analysis by the DG model. The pH subtracted signals can then be corrected for hang-up (Fig 3B; gray line), as described above, before fitting to the RD model.

Another method that is used to resolve mixed pH and DA signals collected by FSCV is principal component regression (PCR), a chemometrics approach (Heien et al., 2005). However, pH change is not always the sole contributor to the measured signal, which may also be affected by interferents such as background drift and other analytes in solution. Figure 4 shows the PCR-resolved components of the same signal that was pH-corrected in Figure 3. The raw FSCV signal (black line), which reflects contributions from multiple analytes, is resolved into its principal components by PCR, to obtain DA (red line), pH (blue line), and background drift (green line). The DA trace resolved from the PCR can be subsequently used for hang-up correction (gray line).

Restricted diffusion model with hang-up correction produces better fits

Figure 5 compares a representative analysis of electrically evoked DA signals altered by MOD (300 mg/kg) using the traditional kinetic approach, the DG model, and a new kinetic approach, the RD model with hang-up correction. Recordings in the top panel of Figure 5A show exemplar DA signals elicited by stimulation of the medial forebrain bundle (MFB) and measured by FSCV at a CFM (left panel, pre-drug; right panel, MOD). Pseudo-color plots shown below and the individual voltammograms (inset) collected at the time of peak signal (vertical white lines on the pseudo-color plot) confirm the evoked signal (horizontal white line on the pseudo-color plot) as DA. Administration of MOD, a wake-promoting psychostimulant (*vide infra*), caused a marked increase in the amplitude and broadening of the electrically evoked DA signal as compared to the pre-drug signal. As shown in Figure 5B the RD model with hang-up correction did indeed produce fits that describe data with higher fidelity than the DG model. We subsequently quantitatively compared the effects of MOD, cocaine, and AMPH on electrically evoked DA signals using the DG model and RD model with hang-up correction.

MOD alters DA release and uptake in the dorsal striatum of anesthetized rats

Developed to treat narcolepsy (Bastoji & Jouvet, 1988), MOD is approved for the treatment of sleep-related disorders, such as obstructive sleep apnea and shift-work sleep disorder. Its therapeutic effects have also been investigated for treating the psychiatric disorders of attention deficit hyperactivity disorder (Swanson et al., 2006) and depression, and drug abuse (Anderson et al., 2009; Anderson et al., 2012). Although MOD acts on various neurotransmitter systems, including orexin, serotonin, glutamate, and GABA, its action on DA has gained importance over time. MOD has been classified as a DAT-inhibiting psychostimulant with low abuse potential (Myrick et al., 2004; Deroche-Gamonet et al., 2002). While preventing DA uptake by inhibition

of DAT has been considered to be its primary mode of action, recently MOD has also been shown to activate phasic DA signaling, which is suggested to be an additional mechanism contributing to its clinical effects (Bobak et al., 2016).

We have previously used the DG model to investigate the effects of MOD on electrically evoked phasic DA signals (Bobak et al., 2016). The evoked signals are considered phasic-like because of their resemblance to the naturally occurring phasic DA transients associated with reinforcement learning and elicited by burst firing of DA neurons (Covey et al., 2014). Our study demonstrated that MOD, in a time- and dose-dependent fashion, increased the amplitude of these evoked DA signals and DA release and decreased DA uptake. Data showing the effects of MOD at a dose of 300 mg/kg on DA release and uptake are replicated in Figure 6A and B (left) for the pre-drug condition and 30 and 60 min post-drug. This data sub-set was statistically re-analyzed using two-way repeated measures ANOVA for the present study. In excellent agreement with Bobak et al. (2016), there was a significant drug-by-time interaction for $[DA]_p$ ($F_{2,18} = 20.19$, $p < 0.0001$), which is the index of DA release, and k ($F_{2,18} = 14.73$, $p = 0.0002$), the first-order rate constant for DA uptake. Post hoc tests also demonstrated that MOD significantly increased $[DA]_p$ ($p < 0.0001$ at 30 and 60 min) and decreased k (30 min: $p = 0.016$; 60 min: $p = 0.0004$), at both time points after drug administration.

We analyzed the same electrically evoked DA signals with the RD model and hang-up correction to determine the effects of MOD on DA release and uptake (Figure 6) and also used two-way repeated measures ANOVA for statistical comparisons. A significant drug-by-time interaction on R_p ($F_{2,18} = 17.62$, $p < 0.0001$), the term for DA release, and k_U ($F_{2,18} = 3.68$, $p = 0.0456$), the term for DA uptake, was seen for the 3-parameter fit (Fig. 6A and B, middle). Similar effects were observed on R_p ($F_{2,18} = 16.85$, $p < 0.0001$) and k_U ($F_{2,18} = 7.74$, $p = 0.0038$) for the 4-

parameter fit (Fig. 6A and B, right). The 4-parameter fit of the RD model is the 3-parameter fit (i.e., R_p, k_U, and k_T, the transport rate constant between compartments) with the addition of k_R, a rate constant reflecting short-term changes in DA release (see Figure 1 and Methods for details). Post hoc tests showed a significant MOD-induced increase in R_p compared to vehicle at 30 (p = 0.0003) and 60 min ($p < 0.0001$) for the 3-parameter fits (Fig. 6A, middle). Similar results were seen for increased R_p with the 4-parameter fits at 30 (p = 0.0012) and 60 min ($p < 0.0001$) post-MOD (Fig. 6A, right). As shown in Figure 6B (middle), 3 parameter-fits showed a significant MOD-induced decrease in k_U compared to vehicle at both time points post-drug (30 min: p = 0.0456 and 60 min: p = 0.0197). However, the 4-parameter fits for k_U (Fig. 6B, right) showed a significant difference from vehicle only at 60 min post-drug (p = 0.0043).

Overall, we did not observe any significant changes in the other two parameters, k_T, the transport rate constant between compartments, and k_R, the rate constant reflecting short-term changes in DA release (Fig. S1). Thus, our results with the RD model concur with Bobak et al. (2016), which used the DG model, and support the notion that not only does MOD decrease DA uptake, it also increases exocytotic DA release.

Fitting of PCR-treated data

The electrically evoked DA signals collected pre-drug and 30-min post-MOD and described above were used to assess whether PCR processing with hang-up correction altered analysis by the RD model (Fig. 7). These data were statistically analyzed using two-way repeated measures ANOVA. Similar to unprocessed data, PCR-treated data showed a significant drug-by-time interaction for R_p with the 3-parameter fit (Fig. 7A, left; $F_{1,6}$ = 23.25, p = 0.0029) and 4-parameter fit (Fig. 7A, right; $F_{1,6}$= 21.6, p = 0.0035), and for k_U with the 3-parameter fit (Fig. 7B, left; $F_{1,6}$ = 22.4, p = 0.0032) and 4-parameter fit (Fig. 7B, right; $F_{1,6}$ = 22.14, p = 0.0033). Post hoc

tests showed a significant increase in R_p (3-parameter fit: $p = 0.0015$, 4-parameter fit: $p = 0.0039$, Figure 7A, right and left, respectively). PCR-treated signals also showed a significant decrease in k_U (3-parameter fit $p = 0.0062$, 4-parameter fit: $p = 0.0062$, Figure 7B, left). Taken together, these results suggest that PCR processing of raw FSCV signals is appropriate for the analysis of DA release and uptake parameters using the RD model.

AMPH alters DA release and uptake in the dorsal striatum of freely behaving rats

The psychostimulant AMPH is a potent DAT-inhibitor that competitively blocks DA uptake and also causes non-exocytotic DA efflux through DAT reversal (Kuczenski and Segal, 1994; Fleckenstein at al., 2007). Historically, high-dose AMPH is thought to disrupt phasic DA signaling, the action potential-dependent transient increases in extracellular DA levels elicited by burst firing of DA neurons (Schultz, 2007), by depletion of vesicular stores of DA, which in turn compromises exocytotic DA release (Hyman et al., 2006; Sulzer, 2011). However, conflicting reports regarding AMPH action have previously been obtained from *in vitro* (Jones et al., 1998; Schmitz et al., 2001) and *in vivo* (Kuhr et al., 1985; May et al., 1988) preparations, as well as from microdialysis (Carboni et al., 1989; Kuczenski et al., 1991) and voltammetric studies (Wiedemann et al., 1990). The basis for these discrepant results is difficult to fully understand, but it should be considered that the *in vivo* preparation better replicates natural physiological responses and that microdialysis suffers from the disadvantages of low temporal resolution and a large probe that damages adjacent tissue, making it difficult to quantify DA levels. More recently, we have used FSCV at a CFM *in vivo* to study AMPH effects on striatal DA signaling and demonstrated that a high dose (10 mg/kg) robustly increased exocytotic DA release and decreased DA uptake in both anesthetized (Ramsson et al., 2011) and freely behaving (Daberkow et al., 2013) rats.

A sub-set of data previously collected in the dorsal striatum of freely behaving rats during pre-drug recording and 5, 10, and 15 min post-AMPH (10 mg/kg) and analyzed with the DG model (Daberkow et al., 2013) is replicated in Figures 8A and B (left). These data were statistically re-analyzed using two-way repeated measures ANOVA. In excellent agreement with Daberkow et al. (2013), these results demonstrated a significant drug-by-time interaction for $[DA]_p$ ($F_{3,24} = 108$, $p < 0.0001$), representing DA release (Fig. 8A left), and k ($F_{3,24} = 18.37$, $p < 0.0001$), representing DA uptake (Fig. 8B, left). AMPH also increases $[DA]_p$ and decreased k at every time point ($p < 0.05$).

We used the 3- and 4-parameter fits of the RD model (Figs. 8A and B, middle and right, respectively) and two-way repeated measures ANOVA to assess the same data. Statistical analyses showed a significant drug-by-time interaction for R_p with the 3-parameter fit (Fig. 8A, middle; $F_{3,24} = 49.75$, $p < 0.0001$) and 4-parameter fit (Fig. 8A, right; $F_{3,24} = 17.2$, $p < 0.0001$), and for k_U with the 3-parameter fit (Fig. 8B, middle; $F_{3,24} = 24.97$, $p < 0.0001$) and 4-parameter fit (Fig. 8B, right; $F_{3,24} = 7.71$, $p = 0.001$). Post hoc tests showed that AMPH significantly increased R_p and decreased k_U at all time points after drug administration for both the 3- and 4-parameter fits ($p < 0.0001$). While we did not observe any significant changes in the k_R for the 4-parameter fit, k_T was significantly decreased for both the 3- and 4-parameter fits (Fig. S2; also see next section). The present analysis with the RD model is thus consistent with our previous analysis using the DG model (Daberkow et al., 2013) and supports the conclusion that in addition to mechanisms such as DA uptake inhibition, DAT reversal, and DA efflux, AMPH elevates extracellular DA in the brain through exocytotic DA release.

AMPH and cocaine alter DA release and uptake in the dorsal striatum of anesthetized rats

We have previously compared the effects of cocaine, which is not thought to deplete vesicular DA stores, and AMPH, which historically is thought to deplete vesicular DA stores, to better understand our paradoxical results showing AMPH enhancing exocytotic DA release in awake rats (Daberkow et al., 2013). Overall, these studies demonstrated that both cocaine and AMPH activated phasic dopamine signaling in the form of DA transients, increased DA release, and decreased DA uptake in the dorsal striatum of anesthetized rats (Ramsson et al., 2011; Covey et al., 2013). Thus, in contrast to the widely accepted view that AMPH and cocaine elicit opposite effects on exocytotic DA release and phasic DA signaling, data from our lab showed that augmentation of action-potential dependent, vesicular DA release was a common property of both psychostimulants.

A sub-set of data from Covey et al. (2013) and showing the effects of AMPH (10 mg/kg) and cocaine (40 mg/kg) on DA release and uptake in anesthetized rats as determined by the DG model is replicated in Figures 9A and B, respectively (left). These data were statically re-analyzed using two-way repeated measures ANOVA. Consistent with Covey et al. (2013), these results demonstrated a significant drug-by-time interaction for $[DA]_p$ ($F_{2,16} = 30.89$, $p < 0.0001$), representing DA release (Fig. 9A top left), and k ($F_{2,16} = 234.1$, $p < 0.0001$), representing DA uptake (Fig. 9A and B, left). Both psychostimulants significantly increased $[DA]_p$ and decreased k compared to saline controls ($p < 0.05$). 3- and 4-parameter RD fits of these same data revealed a significant drug-by-time interaction for the 3-parameter (Fig. 9a, top middle: $F_{2,16} = 46.3$; $p < 0.0001$) and 4-parameter (Fig. 9B, right: $F_{2,16} = 8.36$; $p = 0.0033$) fit of R_p and for the 3-parameter (Fig. 9B, middle: $F_{2,16} = 771.53$; $p < 0.0001$) and 4-parameter (Fig. 9B, right: $F_{2,16} = 664.78$; $p = < 0.0001$) fit of k_U. Both AMPH and cocaine significantly increased R_p ($p = 0.0002$) and decreased

k_U ($p < 0.001$) compared to saline in the 3-parameter data fits. Similarly, statistical analysis of the 4-parameter fits showed that R_p was significantly increased by AMPH ($p = 0.0117$) and cocaine ($p = 0.0302$), and k_U was significantly decreased by AMPH ($p = 0.0025$) and cocaine ($p = 0.0205$). Overall, we also did not observe any significant changes in the other two parameters, k_T and k_R (Fig. S3). The lack of significant effects of AMPH on k_T for either the 3- or 4-parameter fits in these data collected in anesthetized rats is at odds with significant decreases in k_T for data collected in awake rats (Fig. S3). While the origin of this difference is not known, it is interesting to speculate the movement in the awake rat may have created an additional diffusion path that was expressed as a decrease in k_T. Taken together, our results with the RD model thus further support the hypothesis that both cocaine and AMPH act similarly to increase exocytotic DA release and inhibit DA uptake.

METHODS

Data

Data for analyses are from our previously published studies. MOD data (anesthetized rats) were from Bobak et al. (2016; 300 mg/kg, n = 6; vehicle, n = 5). AMPH data (freely behaving rats) were from Daberkow et al. (2013; AMPH = 10 mg/kg, n = 6; saline, n = 6). AMPH and cocaine data (anesthetized rats) were from Covey et al. (2013; AMPH = 10 mg/kg, n= 7; cocaine = 40 mg/kg, n = 5; saline, n = 7). With the exception of the study conducted by Daberkow et al. (2013), which investigated effects in the dorsal striatum, Bobak et al. (2016) and Covey et al (2013) examined dorsal as well as the ventral striatum. However, for the purpose of this investigation, we restricted our analyses to data obtained from the dorsal striatum only.

Animals

For all the three studies mentioned, adult Sprague-Dawley rats (250-300g) were used. Animals were purchased from Harlan (Indianapolis, IN, USA), and housed in a light-, and temperature-controlled vivarium. Access to food and water was provided *ad libitum*. All procedures were in accordance with the *National Institutes of Health Guide for the Care and Use of Laboratory Animals* and approved by the Institutional Animal Care and Use Committee of Illinois State University.

Surgery

For the anesthetized studies, adult male Sprague-Dawley rats were anesthetized with urethane (1.6 g/kg) and mounted in a stereotaxic apparatus. An incision of the scalp was made, and skin and fascia removed. Holes were drilled into the skull to implant recording electrodes, one stimulating electrode, and one reference electrode. Using stereotaxic coordinates relative to bregma (Paxinos & Watson, 1986), the stimulating electrode was placed in the MFB (-4.6 AP, +1.4 ML, -7.0 DV), a CFM was placed in the dorsal striatum (+1.2 AP, +3.0 ML, -4.5 DV), and the Ag/AgCl reference electrode was placed in the contralateral cortex. The stimulating electrode and CFM were lowered and optimized to produce a robust electrically evoked DA signal. The position of the electrodes was fixed for the duration of the experiment after optimization. For the freely behaving studies, rats were anesthetized with ketamine (80 mg/kg) and xylazine (60 mg/kg) injected i.p. before mounting in a stereotaxic frame. Reference and stimulating electrodes and a hub to house a micromanipulator were implanted and secured to the skull. During recording in awake rats, a fresh CFM was lowered after attaching the micromanipulator and optimized prior to the beginning of the experiment. For both studies, the CFMs were prepared by aspirating a single carbon fiber (r = 3.5 μm) into a borosilicate capillary tube and pulling to a taper. A chloridized

silver wire was used as reference electrode. Twisted bipolar stimulating electrodes, with tips spaced ~1 mm apart, were used. Stimulus pulses were optically isolated and delivered at a constant current as 60-Hz, 24-pulse trains at a current intensity of ±300 μA.

FSCV

Electrically evoked dopamine levels were recorded using FSCV at a CFM. A triangular waveform (-0.4 to 1.3 V and back, 400 V/s) was applied every 100 ms. An EI400 bipotentiostat (Ensman Instruments, Bloomington, IN, USA), which was computer controlled using TarHeel-1 software (ESA, Chelmsford, MA, USA), was used to perform FSCV. The CFM was calibrated in TRIS buffer after each experiment to convert the peak oxidation current for DA in each scan to a concentration (Wightman et al., 2007).

Data Analysis

Electrically evoked DA signals were analyzed to determine parameters for exocytotic DA release and DA uptake using two kinetic models:

1. Diffusion gap model (Fig. 1A). This model postulates that brain extracellular DA is governed by the balance between dopamine released and that which is taken back up. To be measured, DA must diffuse across a gap between the CFM and releasing DA terminals. The mathematical equation describing this is as follows (Wightman et al., 1988; Wu et al., 2001):

$$\frac{\mathrm{d[DA]}}{\mathrm{d}t} = [\mathrm{DA}]_{\mathrm{p}} f - k[\mathrm{DA}] \qquad (1)$$

where, $[\mathrm{DA}]_{\mathrm{p}}$ is the concentration of DA released per stimulus pulse, f is the frequency of stimulation, and k is the first-order rate constant for DA uptake. Curve fitting of data to Eq. 1 used non-linear regression with a simplex minimization algorithm. (Wu et al., 2001). Calculated curves were convoluted with an impulse response function for thin layer diffusion prior to data comparison (Kawagoe et al., 1992).

2. Restricted diffusion model (Fig. 1B). This model divides the brain extracellular space into an inner and an outer compartment, and postulates that DA released into the inner compartment diffuses in a restricted manner into the outer compartment, from where it can be measured by the CFM and is subject to reuptake. The model comprises two equations (Walters et al., 2015):

$$\frac{\mathrm{dDA_{ic}}}{\mathrm{d}t} = R_\mathrm{p} f \, \mathrm{e}^{-k_\mathrm{R} t} - \mathrm{DA_{ic}} k_\mathrm{T} \qquad (2)$$

$$\frac{\mathrm{d[DA]_{oc}}}{\mathrm{d}t} = \frac{\mathrm{DA_{ic}} k_\mathrm{T}}{V_\mathrm{oc}} - \mathrm{[DA]_{oc}} k_\mathrm{U} \qquad (3)$$

where $\mathrm{DA_{ic}}$ is the amount (in moles) of DA in the inner compartment, R_p is the moles of DA released per stimulus pulse, f is the stimulus frequency, k_R is a first-order rate constant that signifies modification of DA release by either short-term depression or facilitation, k_T is a first order rate constant for DA transport from inner to outer compartment, V_oc is the volume of the outer compartment (fixed at 16 μm^3) (Walters et al., 2014; Walters et al., 2015; Moss & Bolam, 2008), and k_U is the first-order rate constant for DA uptake.

Hang up correction

Before analyses using the RD model, the effect of hang-up was removed from electrically evoked DA signals by using a correction as explained in detail by Walters et al. (2015). Briefly, the algorithm calculates a hang-up component in terms of first-order rate constants describing the balance between DA adsorption to and desorption from the CFM surface. The equation that describes this balance is as follows:

$$\frac{\mathrm{d}H}{\mathrm{d}t} = k_{\mathrm{on}}C - k_{\mathrm{off}}\Gamma_{\mathrm{DA}} \qquad (4)$$

where k_{on} and k_{off} are first-order rate constants for DA adsorption and desorption, respectively, and C is the concentration of DA in solution in close contact with the electrode, which is the same as the concentration detected by FSCV (Walters et al., 2015). The calculated hang-up component is then subtracted from the measured evoked response, to give a corrected signal.

A brute-force algorithm was used for curve fitting as described in Walters et al. (2015) and Walters et al. (2014). Curve fitting was used to set the values of the adjustable parameters in the hang-up (Eq. 4) and DA kinetic (Eqs. 2 and 3) models. The parameters producing the best fit to data were those that were defined by high Pearson correlation coefficients and the smallest values of the sum of squares of the residuals.

pH correction

The effect of basic pH shifts following electrical stimulation, caused by changes in local blood flow, was removed by using the voltammogram of the pH change occurring a few seconds (~5 s) after stimulation and free of DA. Current for pH (measured typically at ≈-0.2 mV) was then adjusted for the DA oxidative potential (≈+0.6 mV typically) before subtracting the pH current from the total current measured at the DA oxidative potential.

PCR

For PCR, different number of stimulation pulses (12, 24, 48, 60, and 72 pulses), which produce different electrically evoked DA concentrations, were used to construct *in vivo* training sets. From these recordings, five background-subtracted voltammograms for each analyte, DA, pH, and background drift, were collected, and the principal components, which account for most of the relevant data, were calculated using principal component analysis (PCA). Subsequently, each principal component was translated into the corresponding analyte units using least square regression. Experimental recordings containing unknown sample concentrations were then projected on to the principal components, in order to determine their amplitudes (Hermans et al., 2008; Keithley et al., 2009).

Statistics

When appropriate, data are presented as the mean ± SEM. All statistical analyses were performed using SAS. For the MOD (anesthetized rats) and AMPH (freely-behaving rats) studies, a repeated-measures two-way ANOVA with drug and time as independent variables and time as the repeated measure was used for each parameter. Post hoc comparisons were performed by a Sidak test. Effects of AMPH and cocaine (anesthetized rats) were statistically analyzed using a one-way ANOVA with a Dunnett's post hoc test. Significance was set at $p < 0.05$.

Drugs and Chemicals

Urethane, cocaine hydrochloride, and D-amphetamine was purchased from Sigma (St. Louis, MO, USA). MOD was provided by Research Triangle Institute-National Institute on Drug Abuse, Raleigh, NC. All drugs were administered i.p.

CONCLUSION

The ability to inhibit DA uptake has largely been accepted as the unifying mechanism by which DAT-targeting psychostimulants enhance extracellular brain DA levels and cause many of their behavioral effects (Sulzer, 2011; Fleckenstein et al., 2007). As compared to other psychostimulants in this class, AMPH has been shown to elicit greater extracellular DA concentrations, due to its unique action of reversing the direction of DA transport via DAT and causing DA efflux. While most of the cocaine-like psychostimulants are also known to activate action potential-dependent DA signaling, AMPH has been excluded from causing this effect; instead, AMPH disrupts this type of DA signaling by depleting vesicular DA stores and decreasing exocytotic DA release (Sulzer, 2011; Hyman, 2005). Indeed, non-action potential-dependent DA efflux, driven by the depletion of readily releasable DA stores, has been proposed to be the hallmark of AMPH action in the brain.

Kinetic modeling of electrically evoked DA signals *in vivo*, measured before and after drug administration by FSCV at a CFM, provides valuable information about the effects of DAT-targeting psychostimulant on the presynaptic mechanisms of DA release and uptake (Wightman et al., 1988; Wu et al., 2001). The DG model of kinetic analysis, which attributes the diffusional distortions of lag and overshoot to a gap between DA releasing terminals and the CFM, has been used to quantitatively resolve the release and uptake components of evoked DA signals. With the DG model, previous results obtained by our lab are at odds with the accepted model of AMPH action. Indeed, these studies have failed to demonstrate compromised phasic DA signaling due to disrupted exocytotic DA release with high-dose AMPH and instead have shown increased phasic DA signaling and augmented exocytotic DA release, more consistent with the actions of cocaine and cocaine-like DAT inhibitors (Ramsson et al., 2011; Daberkow et al., 2013; Covey et al., 2013).

Moreover, we have more recently shown that an atypical psychostimulant, MOD, also increases DA release (Bobak et al., 2016). However, drawbacks of the DG model, such as its insufficiency in describing the discordant appearance of lag and overshoot, and the presence of hang-up in DA signals, have rendered its application for DA kinetic analysis debatable, thereby raising questions on the finding of psychostimulants augmenting exocytotic DA release. On the other hand, the RD model, based on the concept of restricted diffusion of released DA and its delayed detection at the CFM, more faithfully describes DA signals in terms of lag, overshoot, and hang-up (Walters et al., 2014; Walters 2015).

This study therefore sought to compare results for the psychostimulants, MOD, AMPH, and cocaine, calculated using the DG model with those obtained using the RD model, with a particular focus on assessing the previously identified psychostimulant-induced increase in DA release. Despite their theoretical differences, both models showed amplified exocytotic DA release and decreased DA uptake for all the psychostimulants tested, the latter in keeping with their well-recognized role as DAT-inhibitors. We speculate that the reasons for the excellent agreement between models is that firstly, all signals fit to the DG model were pre-selected via optimization and placement of CFMs close to the DA releasing terminals, which presumably downplayed the effect of the diffusion gap distorting measured DA signals. Secondly, while the DG model was not coupled to the hang-up correction, this distortion was minimized by fitting the early portions of the signals and avoiding the latter portions reflecting the greatest hang-up component.

The major conclusion resulting from this study is that the DAT-targeting psychostimulants, AMPH, cocaine, and MOD, elevate extracellular DA concentration not solely by DA uptake inhibition, but also by upregulating action potential-dependent DA release. This

result is of particular significance with regards to AMPH action, which has historically been considered to elevate extracellular DA levels in the brain primarily by vesicular DA depletion driving DA efflux. We thus propose that DAT inhibitors are misnamed, because this group of psychostimulants may also enhance DA release. Cellular mechanisms of how these psychostimulants increase exocytotic DA release have been investigated. Cocaine has been shown to mediate its effects of enhancing DA release by mobilizing synapsin-bound DA vesicles, which are part of the long-term storage pool (Venton et al., 2006). MPH causes upregulated DA release via α-synuclein, a protein involved in vesicular trafficking (Chadchankar et al., 2012). That AMPH may act also exert its effects on synaptic proteins is a speculation worth testing. Previously results from our lab have demonstrated that AMPH also augments exocytotic DA release by increasing DA synthesis and inhibiting DA degradation, presumably leading to increased cytosolic DA and vesicular loading (Avelar et al., 2013).

Augmentation of vesicular DA release is especially important for activation of the DA transients of phasic DA signaling, which play a critical role in reinforcement learning, goal-directed behavior, and drug addiction (Stuber et al., 2005). Evidence from AMPH and MOD studies shows that enhanced DA release tracks increases in $[DA]_{max}$, the maximal amplitude of electrically evoked phasic-like DA signals, better than reduced DA uptake (Bobak et al., 2016; Covey, et al., 2013; Daberkow, et al., 2013). Assuming that electrically evoked phasic-like DA signals mimic naturally occurring DA transients, a higher correlation of $[DA]_{max}$ with exocytotic DA release compared to DA uptake indicates that increased exocytotic DA release may be responsible for the increased amplitude of DA transients with psychostimulants (Stuber et al., 2005; Daberkow et al., 2013). The augmentation of exocytotic DA release causing the increased amplitude of DA transients may therefore be an important action mediating the abuse potential of

addictive drugs. Hence, this study contributes towards establishment a new unifying mechanism of action of psychostimulants in activating phasic DA signaling through increased exocytotic DA release, in addition to inhibition of DA uptake. This study also highlights the need to reconsider and re-assess mechanisms of action of psychostimulants. While most such drugs are potentially abusive, many are also used as medication. For example, MOD is a commonly prescribed wake-promoting agent (Wise et al., 2007), and AMPH and MPH are used in the treatment of attention deficit hyperactivity disorder (Swanson et al., 1995). Therefore, it is imperative that a detailed understanding of ways in which these drugs act should be explored and elaborated further, in order to aid in better drug development and to improve efforts towards controlling drug abuse.

REFERENCES

1. Anderson, A. L., Li, S. H., Biswas, K., McSherry, F., Holmes, T., Iturriaga, E. et al. (2012). Modafinil for the treatment of methamphetamine dependence. *Drug and alcohol dependence, 120,* 135-141.
2. Anderson, A. L., Reid, M. S., Li, S. H., Holmes, T., Shemanski, L., Slee, A. et al. (2009). Modafinil for the treatment of cocaine dependence. *Drug and alcohol dependence, 104,* 133-139.
3. Avelar, A. J., Juliano, S. A., & Garris, P. A. (2013). Amphetamine augments vesicular dopamine release in the dorsal and ventral striatum through different mechanisms. *Journal of neurochemistry, 125,* 373-385.
4. Bastoji, H. & Jouvet, M. (1988). Successful treatment of idiopathic hypersomnia and narcolepsy with modafinil. *Progress in neuro-psychopharmacology and biological psychiatry, 12,* 695-700.
5. Bobak, M. J., Weber, M. W., Doellman, M. A., Schuweiler, D. R., Athens, J. M., Juliano, S. A. et al. (2016). Modafinil activates phasic dopamine signaling in dorsal and ventral striata. *Journal of Pharmacology and Experimental Therapeutics, 359,* 460-470.
6. Carboni, E., Imperato, A., Perezzani, L., & Di Chiara, G. (1989). Amphetamine, cocaine, phencyclidine and nomifensine increase extracellular dopamine concentrations preferentially in the nucleus accumbens of freely moving rats. *Neuroscience, 28,* 653-661.
7. Chadchankar, H., Ihalainen, J., Tanila, H., & Yavich, L. (2012). Methylphenidate modifies overflow and presynaptic compartmentalization of dopamine via an alpha-synuclein-dependent mechanism. *Journal of Pharmacology and Experimental Therapeutics, 341,* 484-492.
8. Covey, D. P., Juliano, S. A., & Garris, P. A. (2013). Amphetamine Elicits Opposing Actions on Readily Releasable and Reserve Pools for Dopamine. *Plos One, 8*.

9. Covey, D. P., Roitman, M. F., & Garris, P. A. (2014). Illicit dopamine transients: reconciling actions of abused drugs. *Trends in neurosciences, 37,* 200-210.
10. Daberkow, D. P., Brown, H. D., Bunner, K. D., Kraniotis, S. A., Doellman, M. A., Ragozzino, M. E. et al. (2013). Amphetamine Paradoxically Augments Exocytotic Dopamine Release and Phasic Dopamine Signals. *Journal of Neuroscience, 33,* 452-463.
11. Deroche-Gamonet, V., Darnaudery, M., Bruins-Slot, L., Piat, F., Le Moal, M., & Piazza, P. (2002). Study of the addictive potential of modafinil in naive and cocaine-experienced rats. *Psychopharmacology, 161,* 387-395.
12. Di Chiara, G. & Imperato, A. (1988). Drugs abused by humans preferentially increase synaptic dopamine concentrations in the mesolimbic system of freely moving rats. *Proceedings of the National Academy of Sciences of the United States of America, 85,* 5274-5278.
13. Fleckenstein, A. E., Volz, T. J., Riddle, E. L., Gibb, J. W., & Hanson, G. R. (2007). New insights into the mechanism of action of amphetamines. *Annu.Rev.Pharmacol.Toxicol., 47,* 681-698.
14. Heien, M. L. A. V., Khan, A. S., Ariansen, J. L., Cheer, J. F., Phillips, P. E. M., Wassum, K. M. et al. (2005). Real-time measurement of dopamine fluctuations after cocaine in the brain of behaving rats. *Proceedings of the National Academy of Sciences of the United States of America, 102,* 10023-10028.
15. Hermans, A., Keithley, R. B., Kita, J. M., Sombers, L. A., & Wightman, R. M. (2008). Dopamine Detection with Fast-Scan Cyclic Voltammetry Used with Analog Background Subtraction. *Analytical Chemistry, 80,* 4040-4048.
16. Hyman, S. E. (2005). Addiction: A Disease of Learning and Memory. *American Journal of Psychiatry, 162,* 1414-1422.

17. Hyman, S. E., Malenka, R. C., & Nestler, E. J. (2006). Neural mechanisms of addiction: the role of reward-related learning and memory. *Annu.Rev.Neurosci., 29,* 565-598.

18. Jones, S. R., Gainetdinov, R. R., Wightman, R. M., & Caron, M. G. (1998). Mechanisms of amphetamine action revealed in mice lacking the dopamine transporter. *The Journal of Neuroscience, 18,* 1979-1986.

19. Jones, S. R., Garris, P. A., & Wightman, R. M. (1995). Different effects of cocaine and nomifensine on dopamine uptake in the caudate-putamen and nucleus accumbens. *Journal of Pharmacology and Experimental Therapeutics, 274,* 396-403.

20. Kawagoe, K. T., Garris, P. A., Wiedemann, D. J., & Wightman, R. M. (1992). Regulation of transient dopamine concentration gradients in the microenvironment surrounding nerve terminals in the rat striatum. *Neuroscience, 51,* 55-64.

21. Keithley, R. B., Heien, M. L., & Wightman, R. M. (2009). Multivariate concentration determination using principal component regression with residual analysis. *Trends in analytical chemistry : TRAC, 28,* 1127-1136.

22. Kuczenski, R., Segal, D. S., & Aizenstein, M. L. (1991). Amphetamine, cocaine, and fencamfamine: relationship between locomotor and stereotypy response profiles and caudate and accumbens dopamine dynamics. *The Journal of neuroscience, 11,* 2703-2712.

23. Kuhr, W. G., Ewing, A. G., Near, J. A., & Wightman, R. M. (1985). Amphetamine attenuates the stimulated release of dopamine in vivo. *Journal of Pharmacology and Experimental Therapeutics, 232,* 388-394.

24. Lee, T. H., Balu, R., Davidson, C., & Ellinwood, E. H. (2001). Differential time-course profiles of dopamine release and uptake changes induced by three dopamine uptake inhibitors. *Synapse, 41,* 301-310.

25. May, L. J., Kuhr, W. G., & Wightman, R. M. (1988). Differentiation of Dopamine Overflow and Uptake Processes in the Extracellular Fluid of the Rat Caudate Nucleus with FastGÇÉScan In Vivo Voltammetry. *Journal of neurochemistry, 51,* 1060-1069.

26. Moquin, K. F. & Michael, A. C. (2009). Tonic autoinhibition contributes to the heterogeneity of evoked dopamine release in the rat striatum. *Journal of neurochemistry, 110,* 1491-1501.

27. Moss, J. & Bolam, J. P. (2008). A dopaminergic axon lattice in the striatum and its relationship with cortical and thalamic terminals. *The Journal of Neuroscience, 28,* 11221-11230.

28. Myrick, H., Malcolm, R., Taylor, B., & LaRowe, S. (2004). Modafinil: preclinical, clinical, and post-marketing surveillanceGÇöa review of abuse liability issues. *Annals of Clinical Psychiatry, 16,* 101-109.

29. Paxinos, G. & Watson, C. (1986). *The rat brain in stereotaxic coordinates*. (second ed.) New York: Academic Press.

30. Ramsson, E. S., Howard, C. D., Covey, D. P., & Garris, P. A. (2011). High Doses of Amphetamine Augment, Rather Than Disrupt, Exocytotic Dopamine Release in the Dorsal and Ventral Striatum of the Anesthetized Rat. *Journal of neurochemistry, 119,* 1162-1172.

31. Robinson, D. L., Venton, B. J., Heien, M. L. A. V., & Wightman, R. M. (2003). Detecting subsecond dopamine release with fast-scan cyclic voltammetry in vivo. *Clinical Chemistry, 49,* 1763-1773.

32. Schmitz, Y., Lee, C. J., Schmauss, C., Gonon, F., & Sulzer, D. (2001). Amphetamine distorts stimulation-dependent dopamine overflow: effects on D2 autoreceptors, transporters, and synaptic vesicle stores. *The Journal of Neuroscience, 21,* 5916-5924.

33. Schultz, W. (2007). Behavioral dopamine signals. *Trends in neurosciences, 30,* 203-210.

34. Seiden, L. S., Sabol, K. E., & Ricaurte, G. A. (1993). Amphetamine: effects on catecholamine systems and behavior. *Annual Review of Pharmacology and Toxicology, 33,* 639-676.

35. Stuber, G. D., Wightman, R. M., & Carelli, R. M. (2005). Extinction of cocaine self-administration reveals functionally and temporally distinct dopaminergic signals in the nucleus accumbens. *Neuron, 46,* 661-669.

36. Sulzer, D. (2011). How Addictive Drugs Disrupt Presynaptic Dopamine Neurotransmission. *Neuron, 69,* 628-649.

37. Sulzer, D., Chen, T. K., Lau, Y. Y., Kristensen, H., Rayport, S., & Ewing, A. (1995). Amphetamine redistributes dopamine from synaptic vesicles to the cytosol and promotes reverse transport. *The Journal of Neuroscience, 15,* 4102-4108.

38. Swanson, J. M., Greenhill, L. L., Lopez, F. A., Sedillo, A., Earl, C. Q., Jiang, J. G. et al. (2006). Modafinil film-coated tablets in children and adolescents with attention-deficit/hyperactivity disorder: results of a randomized, double-blind, placebo-controlled, fixed-dose study followed by abrupt discontinuation. *J.Clin.Psychiatry, 67,* 137-147.

39. Swanson, J. M., McBurnett, K., Christian, D. L., & Wigal, T. (1995). Stimulant medications and the treatment of children with ADHD. In *Advances in clinical child psychology* (pp. 265-322). Springer.

40. Sykova & Nicholson, C. (2008). Diffusion in Brain Extracellular Space. *Physiological Reviews, 88,* 1277.

41. Taylor, I. M., Ilitchev, A. I., & Michael, A. C. (2013). Restricted Diffusion of Dopamine in the Rat Dorsal Striatum. *ACS Chemical Neuroscience, 4,* 870-878.

42. Venton, B. J., Michael, D. J., & Wightman, R. M. (2003). Correlation of local changes in extracellular oxygen and pH that accompany dopaminergic terminal activity in the rat caudateGÇôputamen. *Journal of neurochemistry, 84,* 373-381.

43. Venton, B. J., Seipel, A. T., Phillips, P. E. M., Wetsel, W. C., Gitler, D., Greengard, P. et al. (2006). Cocaine Increases Dopamine Release by Mobilization of a Synapsin-Dependent Reserve Pool. *The Journal of Neuroscience, 26,* 3206-3209.

44. Walters, S. H., Robbins, E. M., & Michael, A. C. (2015). Modeling the Kinetic Diversity of Dopamine in the Dorsal Striatum. *ACS Chemical Neuroscience, 6,* 1468-1475.

45. Walters, S. H., Taylor, I. M., Shu, Z., & Michael, A. C. (2014). A Novel Restricted Diffusion Model of Evoked Dopamine. *ACS Chemical Neuroscience, 5,* 776-783.

46. Wiedemann, D. J., Basse-Tomusk, A., Wilson, R. L., Rebec, G. V., & Wightman, R. M. (1990). Interference by DOPAC and ascorbate during attempts to measure drug-induced changes in neostriatal dopamine with Nafion-coated, carbon-fiber electrodes. *Journal of neuroscience methods, 35,* 9-18.

47. Wightman, R. M., Amatorh, C., Engstrom, R. C., Hale, P. D., Kristensen, E. W., Kuhr, W. G. et al. (1988). Real-time characterization of dopamine overflow and uptake in the rat striatum. *Neuroscience, 25,* 513-523.

48. Wightman, R. M., Heien, M. L., Wassum, K. M., Sombers, L. A., Aragona, B. J., Khan, A. S. et al. (2007). Dopamine release is heterogeneous within microenvironments of the rat nucleus accumbens. *Eur.J.Neurosci., 26,* 2046-2054.

49. Wise, M. S., Arand, D. L., Auger, R. R., Brooks, S. N., Watson, N. F., & American Academy of Sleep Medicine (2007). Treatment of narcolepsy and other hypersomnias of central origin. *Sleep, 30,* 1712-1727.

50. Wu, Q., Reith, M. E., Wightman, R. M., Kawagoe, K. T., & Garris, P. A. (2001). Determination of release and uptake parameters from electrically evoked dopamine dynamics measured by real-time voltammetry. *Journal of neuroscience methods, 112,* 119-133.

CHAPTER II FIGURES

Figure 1

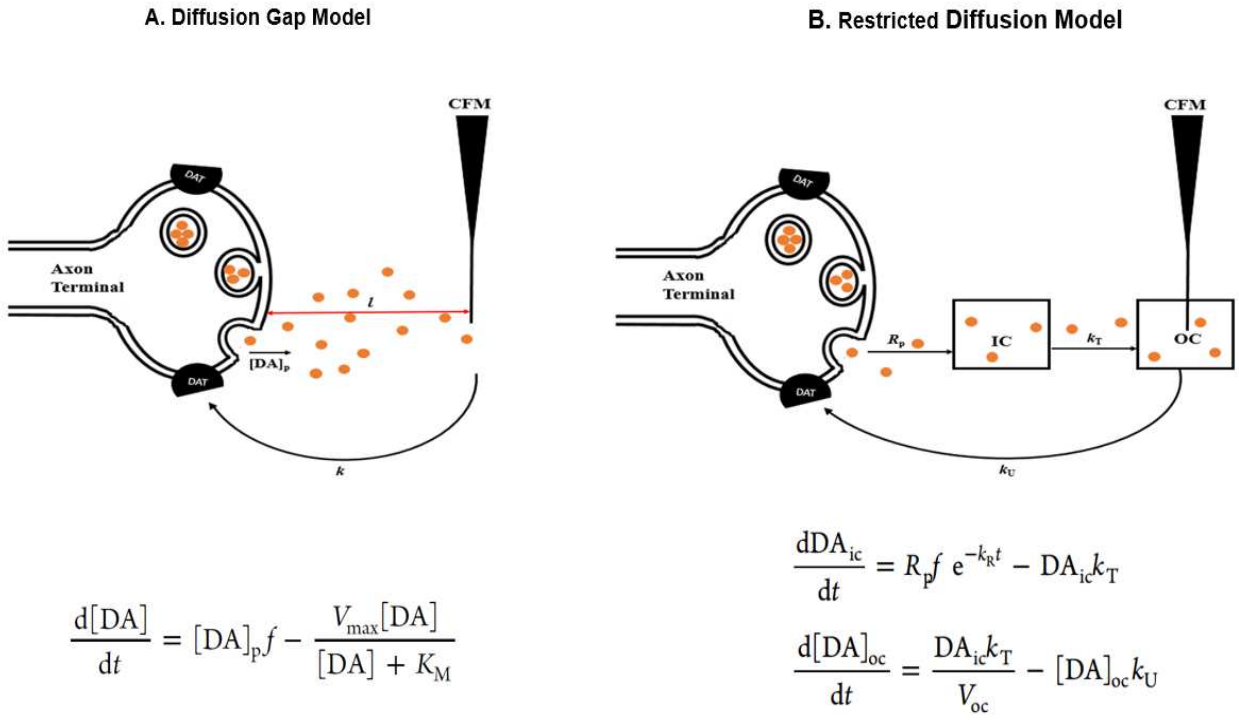

$$\frac{d[DA]}{dt} = [DA]_p f - \frac{V_{max}[DA]}{[DA] + K_M}$$

$$\frac{dDA_{ic}}{dt} = R_p f\, e^{-k_R t} - DA_{ic} k_T$$

$$\frac{d[DA]_{oc}}{dt} = \frac{DA_{ic} k_T}{V_{oc}} - [DA]_{oc} k_U$$

Figure 1. *Schematic representation of DG and RD models.* In the DG model (left panel), released vesicular DA (orange) ($[DA]_p$; f is frequency of stimulation) diffuses through a gap (l), before it reaches the detecting CFM and is cleared by DAT through first-order DA uptake (k). According to Eq. 1, this model describes extracellular DA levels as a balance between DA release and uptake. The RD model (right panel) divides the extracellular space into inner compartment (IC) and outer compartment (OC) and postulates that released DA (R_p; k_R is a first-order rate constant signifying short-term changes in DA release) is transported from IC to OC where DA is measured by the CFM and DA uptake take place. The restricted diffusion of DA and DA uptake are described by the first-order rate constants, k_T and k_U, respectively. The RD model is comprised of two equations (Eqs. 2 and 3), each defining DA levels in the IC and OC, respectively.

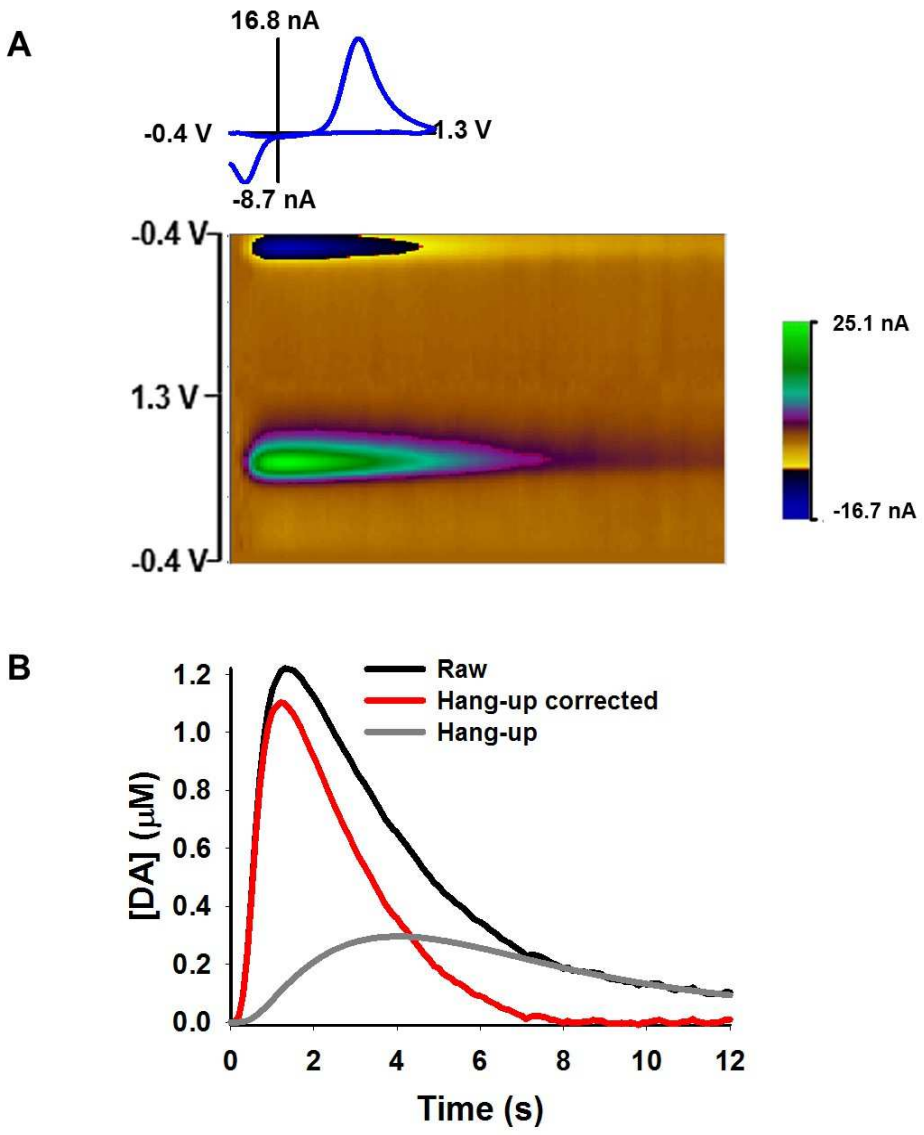

Figure 2. *Hang-up correction of electrically evoked DA signals.* A) Pseudo-color plot of an exemplar electrically evoked DA signal. (Inset) Individual voltammogram (see vertical while line I pseudo-color plot). B) DA concentration obtained from the raw FSCV trace (see horizontal white line in the pseudo-color plot) is displayed in black. The hang-up component (gray) was calculated and subtracted from the raw signal to produce a hang-up corrected DA trace (red).

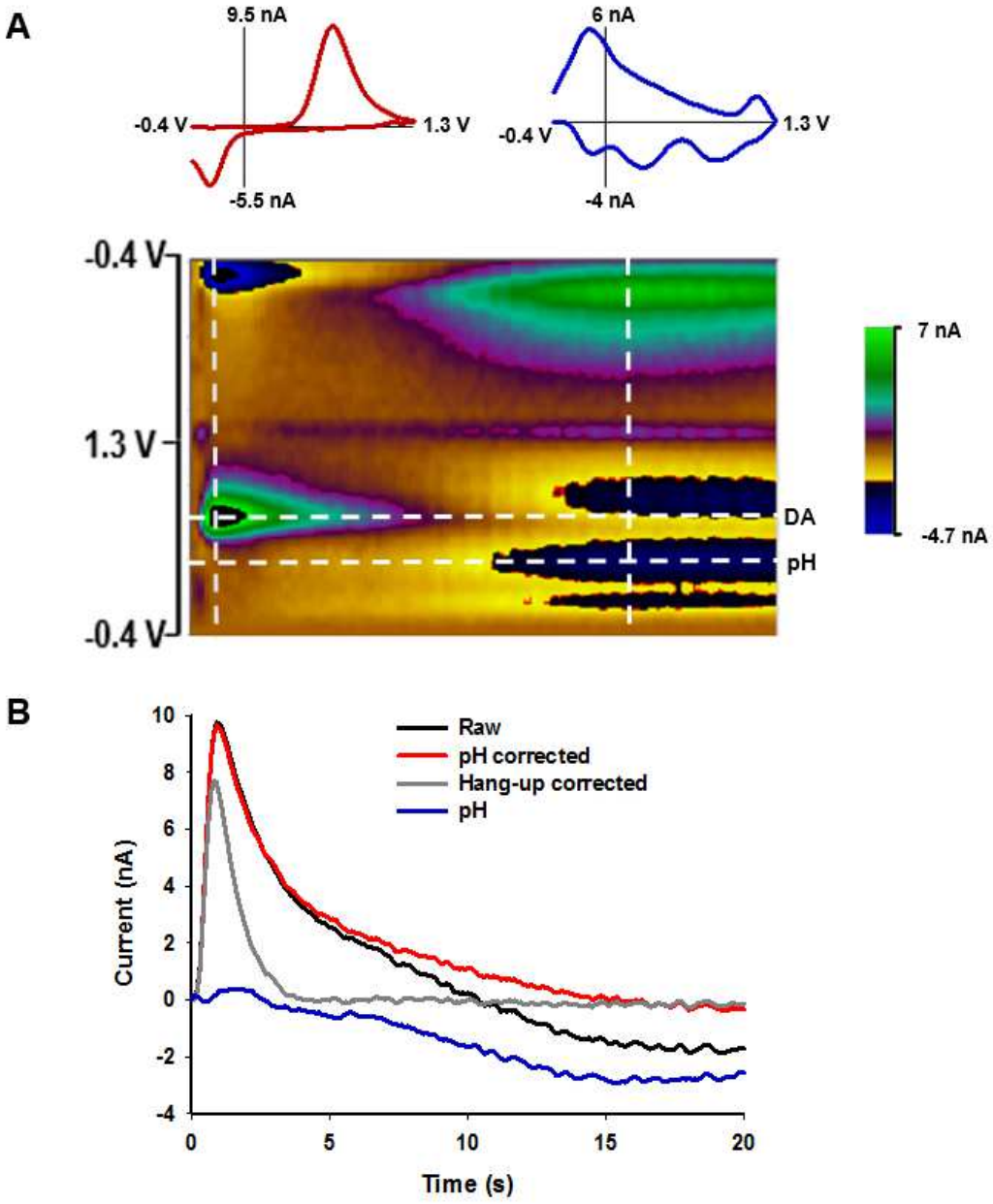

Figure 3. *pH correction of electrically evoked DA signals***.** A) Pseudo-color plot of an exemplar electrically evoked DA signal showing basic pH changes (blue portion). (Inset) Individual voltammograms identify the analytes as DA (red), at the time point represented by the left vertical white line, and pH (blue), at the time point indicated by the right vertical white line of the pseudo-color plot. B) Concentration vs. time plots of the DA trace obtained from raw the FSCV recording (black line; see upper horizontal white line on the pseudo-color plot) and after pH correction (red). The blue line represents the pH current measured at the peak pH potential (see lower horizontal white line on the pseudo-color plot). Hang-up subtracted trace (gray) was obtained by performing hang-up correction on the pH corrected signal.

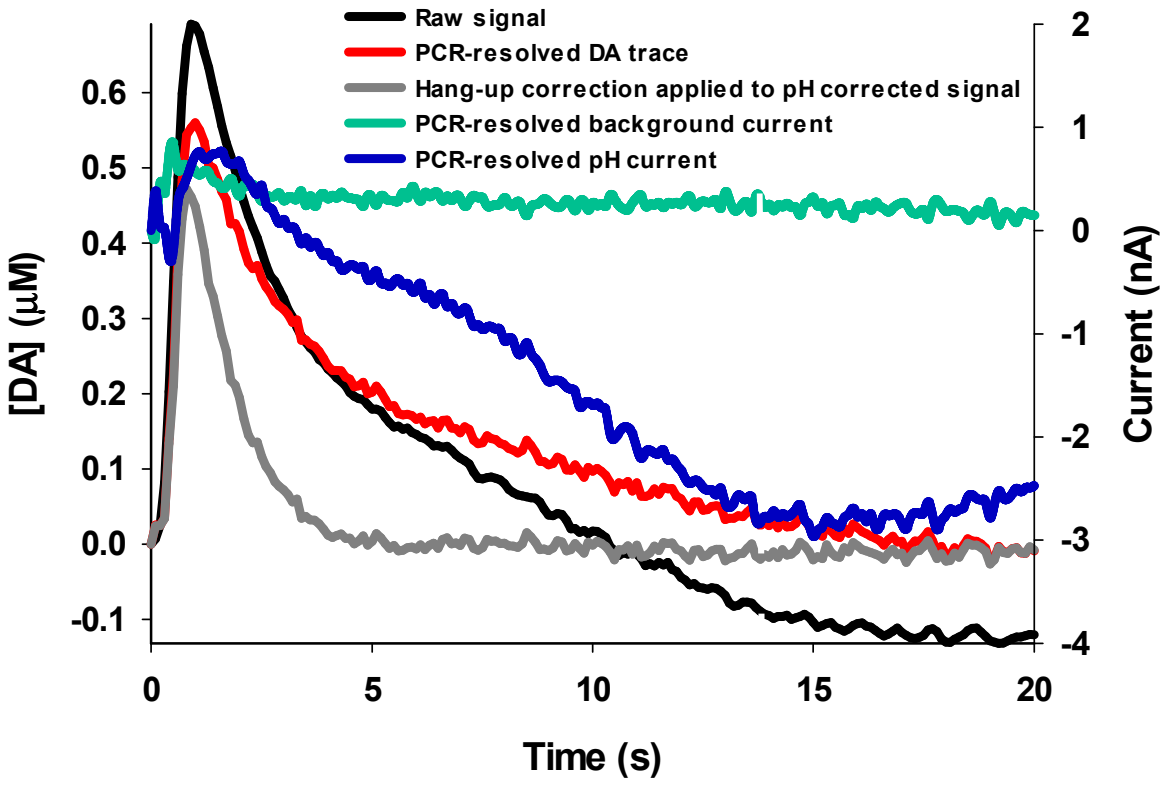

Figure 4. *Hang-up correction of PCR-resolved DA signals.* Concentration vs. time plots of the PCR-resolved DA trace (red) obtained from raw the FSCV recording (black). PCR also resolved the raw signal into principal components for pH (blue) and background drift (green). Hang-up subtracted trace (gray) was obtained by performing hang-up correction on the PCR-resolved DA trace.

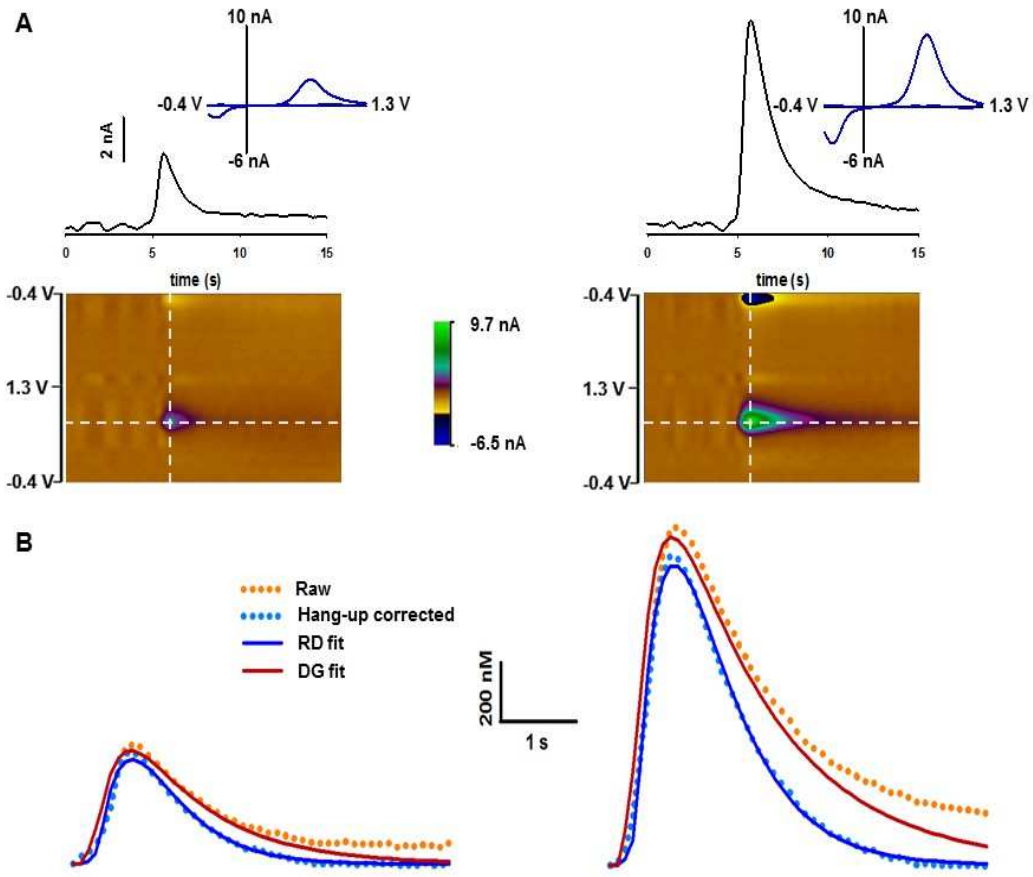

Figure 5. *Comparison of fits obtained by DG and RD models.* A) (Top) DA signals elicited by electrical stimulation before (left) and 60 min after (right) MOD (300 mg/kg) administration. (Inset) Individual voltammograms taken from the peak signal (white vertical line on pseudo-color plots) identifies the analyte as DA. (Bottom) 15-s pseudo-color plots for the pre- and post-MOD evoked signals. White horizontal line identifies the DA peak oxidative potential where the evoked DA trace was collected. B) Fits produced for each of these exemplar signals using the DG (red line) and RD (blue line) models. The DG model was fit to FSCV data (red dots), and the RD model was applied on FSCV data that were hang-up corrected (blue dots).

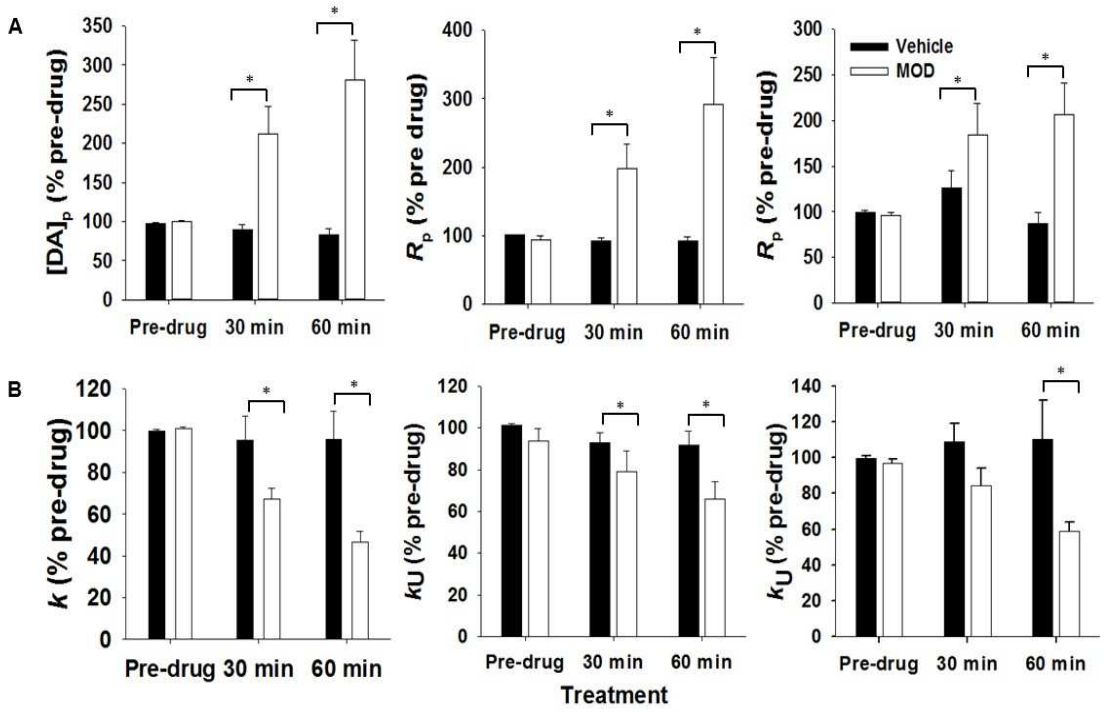

Figure 6. *MOD activates exocytotic DA release and reduces DA uptake.* A) An increase in the DA release parameter from the DG model (left), and the 3-parameter (middle), and 4-parameter (right) fits of the RD model was seen in response to administration of MOD (300 mg/kg). B) MOD causes a decrease in DA uptake as shown by the reduced uptake parameter of the DG (left), and the 3-parameter (middle) and 4-parameter (right) fits of the RD model. Data are expressed as a percent of pre-drug and are the mean ± SEM. Data were analyzed for significance using two-way repeated measures ANOVA ($p < 0.05$).

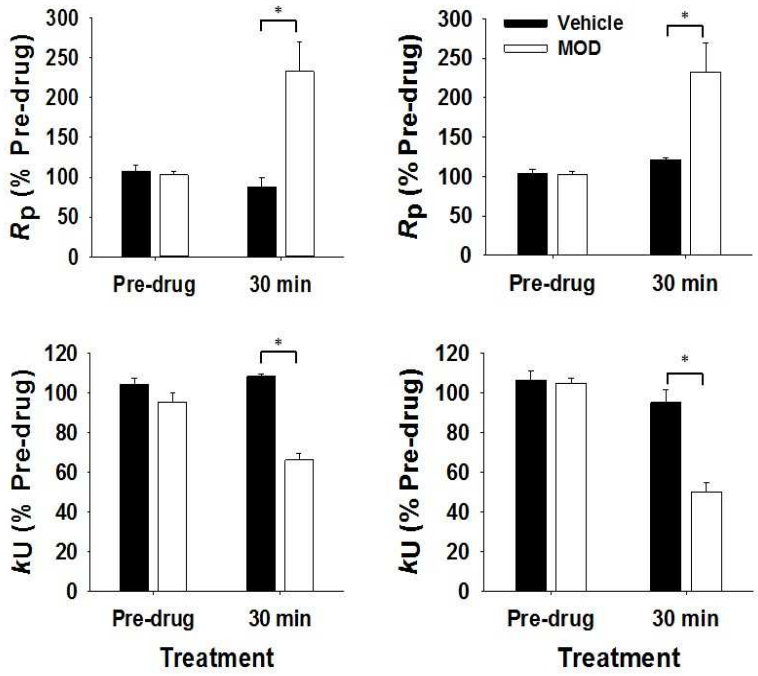

Figure 7. *MOD increases DA release and reduces DA uptake in PCR-treated DA traces.* A) 3-parameter (left) and 4-parameter (right) fits of the RD model showed that MOD increases *R*p at 30 min post-drug. B) 3-parameter (left) and 4-parameter (right) fits of the RD model showed that MOD significantly reduces k_U at 30 min post-drug. Data are expressed as a percent of pre-drug and are the mean ± SEM. Data were analyzed for significance using two-way repeated measures ANOVA ($p < 0.05$).

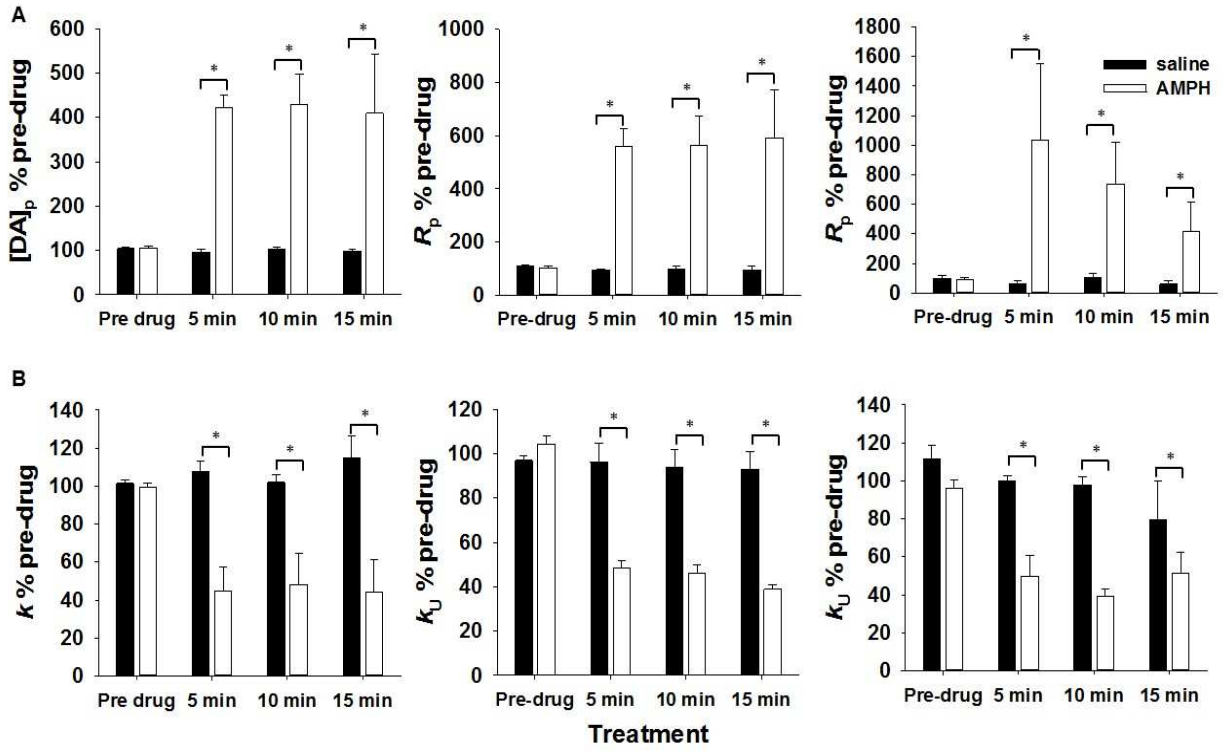

Figure 8. *AMPH activates exocytotic DA release and reduces DA uptake.* A) An increase in the DA release parameter from the DG model (left), and the 3-parameter (middle) and 4-parameter (right) fits of the RD model was seen in response to administration of AMPH (10 mg/kg). B) AMPH caused a decrease in DA uptake as shown in the reduced uptake parameter of the DG model (left), and the 3-parameter (middle) and 4-parameter (right) fits of the RD models. Data are expressed as a percent of pre-drug and are the mean ± SEM. Data were analyzed for significance using two-way repeated measures ANOVA ($p < 0.05$).

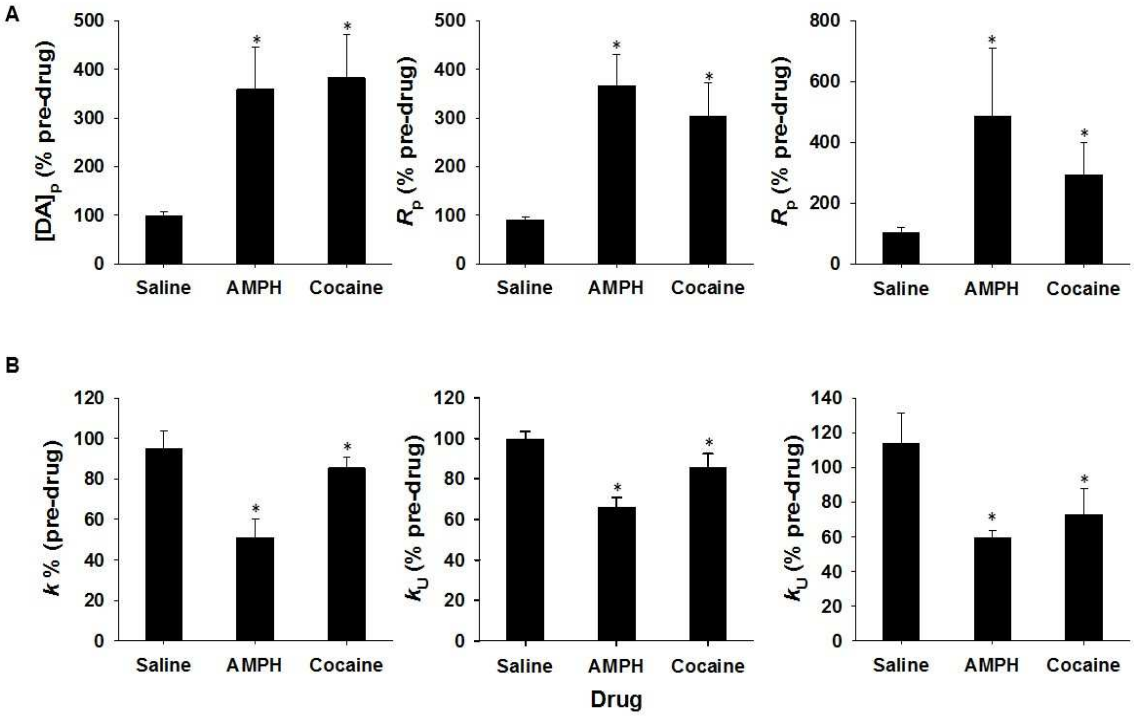

Figure 9. *Comparison of effects of AMPH and cocaine on DA release and uptake.* A) Both AMPH and cocaine significantly increased exocytotic DA release as shown by the increased release parameter of the DG model (left), and 3-parameter (middle) and 4-parameter (right) fits of the RD model. B) AMPH and cocaine reduced DA uptake as shown by the decreased uptake parameter of the DG model (left) and 3-parameter (middle) and 4-parameter (right) fits of the RD model. Data are expressed as a percent of pre-drug and are the mean ± SEM. Data were analyzed for significance using one-way ANOVA ($p < 0.05$).

CHAPTER II SUPPLEMENTARY FIGURES

S1. Two-way repeated measures ANOVA of DA signals altered by MOD (300 mg/kg) and collected in anesthetized rats showed no significant effects of drug, time, and drug-by-time interaction on the parameters k_T from the 3- and 4-parameter fits, and k_R from the 4-parameter fits.

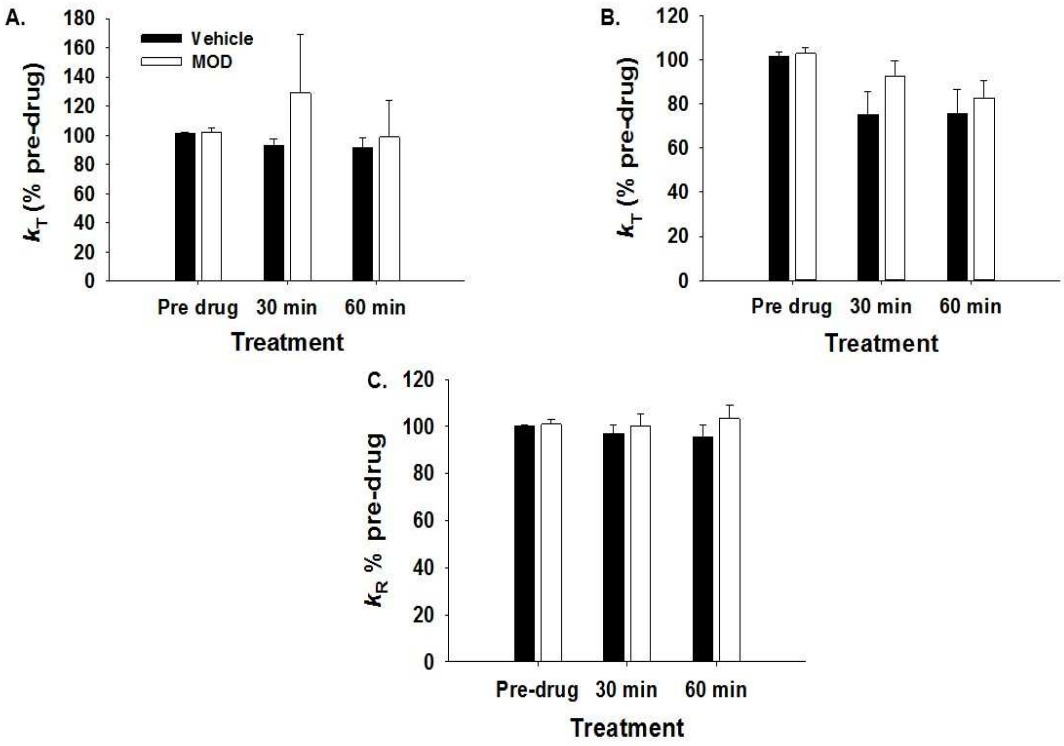

S2. Two-way repeated measures ANOVA of DA signals altered by AMPH (10 mg/kg) and collected in awake rats showed significant effects of drug ($F_{1,32} = 73.05$; $p < 0.0001$), time ($F_{3,32} = 27.06$; $p < 0.0001$), and drug-by-time interaction ($F_{3,32} = 20.00$; $p < 0.0001$) on the parameter k_T for the 3-parameter fits. AMPH was significantly different from vehicle at all time points after drug administration ($p < 0.0001$). 4-parameter fits also showed significant effect of drug ($F_{1,31} = 95.7$; $p < 0.0001$), time ($F_{3,31} = 40.01$; $p < 0.0001$), and drug-by-time interaction ($F_{3,31} = 44.65$; $p < 0.0001$). k_R from the 4-parameter fits did not change significantly.

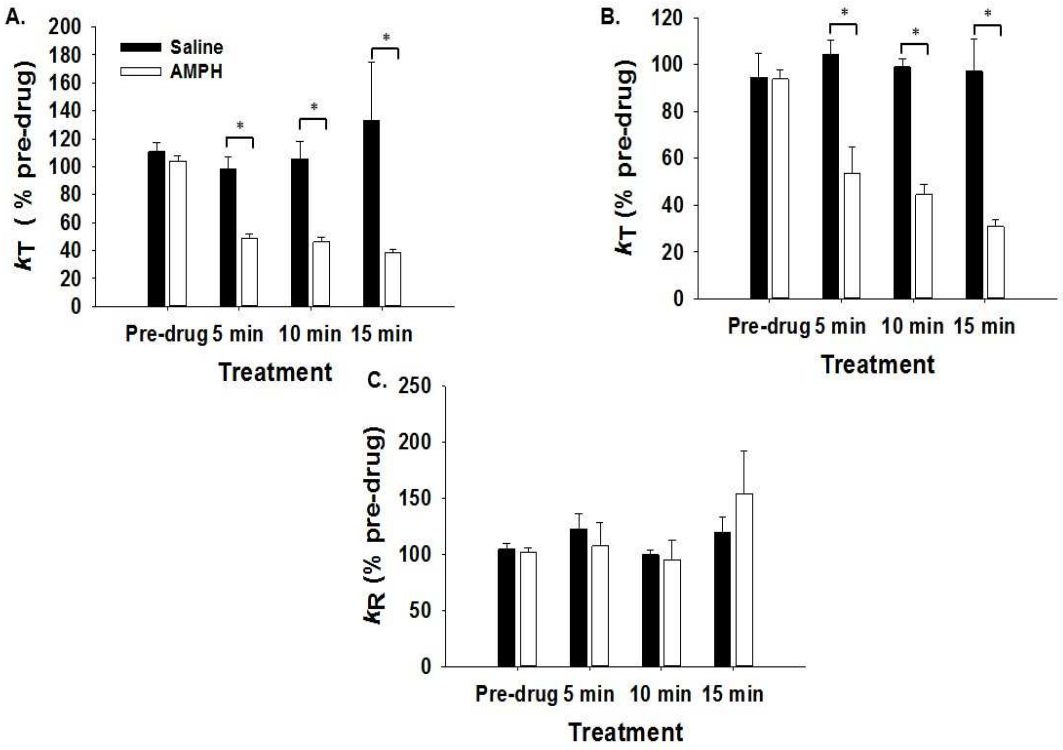

S3. Two-way repeated measures ANOVA of DA signals altered by AMPH (10 mg/kg) and cocaine (40 mg/kg) and collected in anesthetized rats showed no significant effects of drug, time, and drug-by-time interaction on the parameters k_T from the 3- and 4-parameter fits, and k_R from the 4-parameter fits in dorsal striatum of anesthetized rats.